ABSTRACT

A NEW THEORY OF PREMIXED FLAMES IN NEAR-STOICHIOMETRIC MIXTURES

by
Eliana S. Antoniou

In this dissertation, a new model of premixed flames in near-stoichiometric mixtures is derived. Unlike most previous theories, which are valid only for very lean or very rich, i.e. off-stoichiometric conditions, our model remains valid over the entire spectrum of mixture compositions, from lean to rich, including the near-stoichiometric regime. Since fuel-mixture composition is known to have a significant effect on flame behavior, such a model is expected to contribute new insights into classical problems in premixed combustion.

In the first part of this dissertation, we describe the derivation of a model for premixed flames in two-reactant mixtures in a formal asymptotic way. Using the method of matched asymptotics we are able to simplify the complicated governing equations of combustion and effectively decouple the hydrodynamic equations from those of heat and mass transport. Our model considers a two reactant mixture in which one reactant is slightly in excess and the other deficient. We show that, if the initially excess reactant is less mobile, then it doesn't diffuse as rapidly across a strained flow field and can be locally deficient, and hence consumed, at the reaction zone. This can have a significant effect on burning characteristics of the flame. There are two major differences between our model and previous models. First, we have an additional reaction-diffusion equation governing the transport of the second species. Second, the derived conditions relating the gradients across the reaction sheet are shown to take one of two different forms, depending on which of the two species is consumed in the reaction.

In the second part of the thesis, we use our model to study the behavior of planar and strained flames. For the planar flame in uniform flow, we find that many of the results of single-reactant theory apply under near-stoichiometric conditions, provided an effective Lewis number is introduced. On the other hand, for a flame in a non-uniform flow, the dynamics depend significantly on the mass diffusivities as well as mixture strength. In particular, we have analyzed the structure of flame in stagnation point flow and given a complete description of the combustion process including extinction conditions. Results are shown to compare favorably with experiments.

A NEW THEORY OF PREMIXED FLAMES IN NEAR-STOICHIOMETRIC MIXTURES

by
Eliana S. Antoniou

A Dissertation
Submitted to the Faculty of
New Jersey Institute of Technology and
Rutgers, The State University of New Jersey – Newark
in Partial Fulfillment of the Requirements for the Degree of
Doctor of Philosophy in Mathematical Sciences
Department of Mathematical Sciences
Department of Mathematics and Computer Science, Rutgers-Newark

January 2002

APPROVAL PAGE

A NEW THEORY OF PREMIXED FLAMES IN NEAR-STOICHIOMETRIC MIXTURES

Eliana S. Antoniou

Dr. John K. Bechtold, Dissertation Advisor — Date
Associate Professor of Mathematical Sciences, NJIT, Newark NJ

Dr. Michael Booty, Committee Member — Date
Associate Professor of Mathematical Sciences, NJIT, Newark NJ

Dr. Burt Tilley, Committee Member — Date
Associate Professor of Mathematics, Franklin W. Olin College of Engineering, Needham MA

Dr. Dawn A. Lott, Committee Member — Date
Assistant Professor of Mathematical Sciences, NJIT, Newark NJ

Dr. Zoi-Heleni Michalopoulou, Committee Member — Date
Associate Professor of Mathematical Sciences and Department of Electrical and Computer Engineering, NJIT, Newark NJ

BIOGRAPHICAL SKETCH

Author: Eliana S. Antoniou

Degree: Doctor of Philosophy

Date: December 2001

Undergraduate and Graduate Education:

- Doctor of Philosophy in Applied Mathematics,
  New Jersey Institute of Technology and Rutgers University , Newark, NJ, 2001
- Master of Science in Applied Mathematics,
  New Jersey Institute of Technology and Rutgers University , Newark, NJ, 1999
- Bachelor of Arts in Mathematics,
  The College of New Jersey, Trenton,NJ, 1996

Major: Applied Mathematics

Presentations and Publications:

Eliana S. Antoniou,
"Careers in Mathematics,"
Invited Speaker, Passaic County Community College, Paterson, N.J., 2000

E. S. Antoniou and J. K. Bechtold,
"A new theory of premixed flames in near-stoichiometric mixtures," *in preparation*, 2001.

To the Memory of my Brother

ACKNOWLEDGMENT

I would like to thank my advisor, Professor John Bechtold, for being such a wonderful person and educator. He has been very supportive and understanding during the past years, and I feel very lucky and privileged for having him as my advisor. He is a very knowledgeable person, and he has taught me a lot of things in combustion. He has been a great source of motivation, and I really look up to him. Words are not enough to express how appreciative I am for his guidance and invaluable teachings he has shared with me. For that, and also for his kindness, I thank him deeply. He is a person that I respect a lot and admire.

I would also like to thank my Committee members, Professors Booty, Lott, and Michalopoulou for agreeing to be part of my work. I appreciate their input, and I thank them for their constructive comments. Special thanks goes to Professor Burt Tilley for always having the time to discuss and suggest improvements for my work. His comments were always encouraging and I thank him for that.

My gratitude goes to a very good friend of mine, Dr. Amir Yefet, for taking the time to teach me how to use matlab and learn to "like" computers. His input has been of great use to me. Also, I would like to express my deepest appreciation to Dr. Martin Katzen for his continuing support, endless advice and above all for encouraging me to teach.

I would also like to thank my fellow graduate students for being such a wonderful group of friends. We shared a lot together and even though we work in different areas of applied math, we find common ground to discuss and relate our work.

Lastly, I would like to thank my family for being so wonderful. I will always be fascinated with the way they value higher education and have passed that idea to all of my brothers and sisters. Finally, my husband for always being proud of me and praising the importance of the field of applied mathematics.

TABLE OF CONTENTS

LIST OF FIGURES

Figure **Page**

CHAPTER 1

INTRODUCTION

1.1 Motivation and Objective

It is well known that fuel-mixture composition can have a significant effect on flame behavior. For example, flames in light hydrocarbon mixtures are observed to propagate with a smooth surface when the mixture is lean, while the flame surface takes on a cellular appearance when the mixture is rich [1]. Similarly, a great deal of soot formation typically occurs in rich mixtures, while substantially less is produced when the mixture is lean [2]. Many technologies employ combustion as a source of energy, for example engines, furnaces and jets. Important issues regarding efficiency and pollutants depend significantly on the mixture composition.

Despite the recognized importance of mixture strength in practical combustion applications, most theoretical studies are based on single reactant models in which the overall chemical reaction is represented by a one-step irreversible reaction for a single reactant decomposing into products. All other reactants appear in relatively large amounts, and so only a minimal amount is consumed. These models are therefore valid only when the mixture is very lean or very rich, i.e. far from stoichiometric. They don't exhibit any dependence whatsoever on the mixture strength, usually measured in terms of the equivalence ratio, which is the ratio of the mass of fuel to oxidant in the fresh mixture (an equivalence ratio of one corresponds to a stoichiometric mixture). Many practical combustion systems operate in a regime closer to stoichiometry, and as noted above, this is a transition regime where flame dynamics can change dramatically. The subject of this thesis is the development of a new theory of premixed flames that accounts for the entire spectrum of mixture compositions, from lean to rich, including the near-stoichiometric regime.

The equations governing combustion processes are extremely complicated. They consist of equations of heat and mass transport coupled to the equations of hydrodynamics for a viscous compressible fluid. They are also highly nonlinear. Theoretical advances in combustion have been made by extracting, from this full system, reduced models that incorporate much of the essential physics of the problem, but can more easily be analyzed.

The earliest theoretical treatment of premixed flames dates back to Landau [3] and Darrieus [4] who treated the flame as a surface of density discontinuity, separating a burned (less dense) from an unburned (more dense) region of gas. By imposing conditions of mass and momentum conservation across the front, as well as the condition that the front propagate at a constant rate relative to the local underlying flow, they were able to study the stability of a planar flame. They concluded that the flame is unconditionally unstable due to the thermal expansion (density difference) across the flame. However, their model ignores effects of diffusion in the flame structure which are potentially stabilizing.

In more recent years, asymptotic methods have been used to formally derive new models of premixed flames. Since most combustion systems exhibit behavior that takes place over a range of spatial and temporal scales, the method of matched asymptotic expansions has proven to be an especially powerful tool to derive reduced models for these systems. These methods have been used, for example, to derive corrections to the Landau model that include the effects of the flame structure [5, 6]. In these hydrodynamic models, the flame is assumed large relative to its thickness, so that the flame structure is quasi-steady and quasi-one-dimensional. As such, these models allow for the effect of the flame on the flow field, but they ignore the effect of the flow on the flame.

A second class of asymptotic models that have been formally derived are the diffusional-thermal, or constant density, models [7]. These models allow for variations

over spatial scales on the order of the flame thickness. They are derived in the limit of large activation energy, so that the thin reaction zone can be resolved asymptotically, and the nonlinear reaction zone is effectively replaced by jump conditions for the transport variables. Furthermore these treatments also consider weak thermal expansion, or constant density, to decouple the hydrodynamic equations from those of heat and mass transport. In this way these models consider the effect of the flow on the flame but ignore the effect of the flame on the flow. Furthermore, these models treat near-equidiffusional conditions, i.e. the heat and mass diffuse at nearly equal rates.

A third class of models is the Slowly-Varying Flame (SVF) model which is valid when heat and mass diffuse at unequal rates [8]. A formal asymptotic treatment of the flame structure, where slow variations in time and the transverse spatial dimensions are considered, results in a nonlinear equation for the propagation speed of the flame.

All of the models described above have played a major role in advancing theoretical combustion. They have been used to study flame behavior in various geometrical configurations, and they have contributed a great deal to our understanding of premixed flame dynamics. For example, mechanisms for instability have been clearly identified, and other phenomena, such as extinction, have been accurately described. However, they all consider the mixture to be far removed from stoichiometry. As such, all results depend on a single Lewis number, which is the ratio of thermal diffusivity of the mixture to mass diffusivity of the deficient reactant. It has been shown, for example, that an initially smooth flame will lose stability to a cellular surface when this Lewis number is less than a critical value, slightly less than unity. Furthermore, a flame in a nonuniform flow can extinguish when the Lewis number is greater than one but not otherwise. Therefore, predicted behavior of a given mixture can be quite different depending on whether conditions are lean or rich. These models cannot describe the transition from one burning regime to another as stoichiometry is crossed. For conditions close to stoichiometry, both fuel and oxidant can be expected

to play a role in flame characteristics. In this case, both the Lewis numbers as well as the equivalence ratio are important parameters affecting flame response.

Theoretical investigations of stoichiometric, or near-stoichiometric, flames have mostly been limited to planar or perturbed planar flames. The flame speed and flame temperature of planar flames were derived by Sen and Ludford [9] and by Mitani [10]. Those analyses showed that the flame temperature achieves a maximum value at stoichiometry, while the flame speed has a maximum slightly on the rich side of stoichiometry, consistent with experiments. A diffusional-thermal model of perturbed, planar near-stoichiometric flames was considered by Joulin and Mitani [11]. They found that the initially deficient reactant was always consumed by the flame, while a small amount of the abundant species leaks through. The Lewis numbers of both fuel and oxidant, as well as the equivalence ratio, were found to affect stability. However, these parameters combined into an effective Lewis number, and conclusions from the stability analyses of off-stoichiometric flames remained valid near stoichiometry, with the effective Lewis number replacing that of the deficient reactant. A similar conclusion was reached by Sivashinsky [12] who considered a perturbed planar flame at exact stoichiometric conditions. Jackson [13] also found that the only modification to the hydrodynamic model of a perturbed planar flame was the presence of the effective Lewis number. Cui, Matalon and Bechtold [14] have recently shown that hydrodynamic models of flames of arbitrary shape in general flows are modified in a similar way. Although their model can be used to treat nonplanar flames, the structure remains quasi-one-dimensional.

All of the theories of near-stoichiometric flames just mentioned are valid for conditions under which the flame structure is nearly planar, and the Lewis numbers are close to unity. Under these conditions, temperature perturbations behind the flame are very weak. As a result, the initially deficient reactant is always consumed at the front, and the burning characteristics differ only slightly from the planar flame.

However, when the two species and mass diffuse at unequal rates, that is, their Lewis numbers are distinct from unity, or when the flame structure is non-planar (as it is in the diffusional-thermal model) flame behavior is expected to be quite different.

Recently, Bechtold and Matalon [15] derived a new SVF model for two-reactant flames in near-stoichiometric mixtures. They found that, when a flame is strained or curved, the rate at which a reactant reaches the reaction zone is strongly affected by its molecular diffusivity. Further, they showed that it is possible when the initially excess reactant is less mobile (larger Lewis number) it does not diffuse as readily across the strained flow and can be locally deficient, and hence consumed, at the reaction zone. This can have important consequences on the burning characteristics, such as extinction, of curved and strained flames.

Still lacking is a diffusional-thermal model of near-stoichiometric flames, and the main goal of this thesis is to fill that void. This new model is derived in a formal asymptotic way from the full system of equations governing premixed flames in a two-reactant mixture. Similar to the one-reactant theory, the analysis is carried out considering the limits of large activation energy and weak thermal expansion. The former enables the resolution of the nonlinear reaction rate terms, and the latter limit decouples the equations of hydrodynamics from the transport equations. The model explicitly demonstrates the importance of the combined effects of straining and differential diffusion. The model differs from previous models in two crucial ways. First, it consists of an additional coupled equation governing the transport of the second species. Second, the derived jump conditions for the gradients across the reaction sheet can take one of two different forms, depending on which of the two species is ultimately consumed by the reaction. This can lead to quantitative and qualitative differences in predicted flame behavior in strained flow fields.

Our model is expressed in a coordinate-free form that is applicable to flames of arbitrary shapes in general prescribed flow fields. Although the derivation assumes

conditions close to stoichiometry, we recover the single-reactant off-stoichiometric results in the appropriate limit, suggesting the applicability of our model over the complete range of mixture strengths. The model is used to re-examine the burning characteristics of planar and strained flames. We show that it is possible for a perturbed planar flame to have some regions burning fuel-lean while neighboring regions burn fuel-rich. Thus oxidant leaks through the first region, and fuel through the other. Although the predicted dynamics of the premixed flame is the same in both regions, such flames can support a trailing diffusion flame where the fuel and oxidant diffuse together.

The model is also used to study the extinction characteristics of strained flames in non-uniform flows. In particular, the flame in a stagnation point flow is considered. This is the simplest example of a positively stretched flame, i.e. one whose surface area tends to increase as a result of the diverging flow. Such flames are observed to extinguish when the Lewis number of the deficient reactant is sufficiently less than one. Thus, for example, lean propane-air and rich hydrogen-air flames are known to behave in this way. A theoretical description of this problem was given by Buckmaster [16], using one-reactant diffusional-thermal model. Our new theory uncovers some new and interesting results. It is shown that the flame standoff distance as a function of strain rate can either decrease monotonically to the wall (no extinction), or it can exhibit turning point behavior, in which case the flame extinguishes a finite distance from the wall. The nature of these curves depends significantly on which of the two species is ultimately consumed at the reaction zone. For weak stretch, the flame is shown to reside a large distance from the wall and the initially deficient is always consumed. For larger strain rates, however, the disparate diffusivities may result in the initially abundant species to be locally deficient, and hence consumed. In such cases the predicted flame response can be quite different. A complete description of the extinction characteristics of these flames is given.

The thesis is arranged as follows. In chapter 2, we introduce the governing equations and systematically derive the new model. In chapter 3, the extinction of uniformly strained premixed flames in stagnation point flow is studied. Finally, a summary of conclusions and suggestions for future research are presented in chapter 4.

CHAPTER 2

DERIVATION OF A NEW MODEL OF PREMIXED FLAMES

A premixed flame is a wave-like phenomena in which a chemically reacting front propagates through a combustible mixture. In the fresh mixture, fuel and oxidant are mixed at the molecular level prior to reaction. The equations governing this process are very complicated; they consist of equations governing transport of heat and species, coupled to the equations of hydrodynamics. The system is highly nonlinear and no exact solutions exist. However, much combustion phenomena is characterized by rapid variations over very short spatial and temporal scales, and thus asymptotic methods have proven to be a useful tool to analyze these systems. In particular, the method of large activation energy asymptotics has been used to derive from these equations reduced models that capture much of the essential physics but are more readily analyzed. In this chapter, we employ this technique to derive a new model of premixed flames that is valid over a range of mixture strength. In later chapters, the model will be used to study the dynamics of stretched and non-stretched flames.

2.1 Formulation

Consider a premixed combustible mixture, consisting of an excess (E) and deficient (D) reactant, in which reaction proceeds according to:

$$\nu_E \mathcal{M}_E + \nu_D \mathcal{M}_D \rightarrow \text{Products},$$

where $\mathcal{M}_i$ are the chemical symbols for species i and ν_i are the stoichiometric coefficients. An important parameter in this analysis is the equivalence ratio

$$\hat{\Phi} = \frac{Y_F/\nu_F W_F}{Y_O/\nu_O W_O},$$

which is the ratio of the mass of the fuel-to-oxidant reactants in the fresh mixture to their ratio in the stoichiometric mixture. Here Y_i denote the mass fractions of species

i and W_i their molecular weights. Values of $\hat{\Phi}$ larger than unity correspond to fuel rich mixtures, and $\hat{\Phi}$ less than one corresponds to lean mixtures. To avoid discussing lean and rich mixtures separately it is convenient to introduce a new parameter

$$\hat{\phi} = \frac{Y_E/\nu_E W_E}{Y_D/\nu_D W_D},$$

which is the ratio of the masses of excess to deficient reactants. As defined, $\hat{\phi}$ is always greater than one; it is equal to $\hat{\Phi}$ for rich mixtures and $\frac{1}{\hat{\Phi}}$ for lean.

The equations governing the transport of heat and species can be written as:

$$\hat{\rho} c_p \frac{D\hat{T}}{D\hat{t}} - \hat{\nabla} \cdot (\hat{\lambda} \hat{\nabla} \hat{T}) = \hat{Q}\omega \tag{2.1}$$

$$\hat{\rho} \frac{DY_i}{D\hat{t}} - \hat{\nabla} \cdot (\hat{\rho} \mathcal{D}_i \hat{\nabla} Y_i) = -\nu_i W_i \omega \tag{2.2}$$

where $\hat{\rho}$, $\hat{T}$, $\hat{Y}_i$ denote density, temperature and species, respectively. The parameters appearing in these equations include the specific heat, c_p, thermal conductivity, $\hat{\lambda}$, heat release, $\hat{Q}$, and mass diffusivity, $\mathcal{D}_i$. The reaction rate ω obeys an Arrhenius temperature law and it is given by:

$$\omega = B\hat{\rho}^2 \frac{Y_E Y_D}{W_E W_D} e^{\frac{-E}{R^\circ \hat{T}}}, \tag{2.3}$$

where B is the frequency factor, E is the activation energy, and R° the gas constant. These equations are coupled to the Navier-Stokes equations for a viscous, compressible fluid. The continuity and momentum equations are given by:

$$\frac{\partial \hat{\rho}}{\partial \hat{t}} + \hat{\nabla} \cdot (\hat{\rho} \hat{\mathbf{V}}) = 0 \tag{2.4}$$

$$\hat{\rho} \left(\frac{\partial \hat{\mathbf{V}}}{\partial \hat{t}} + \hat{\mathbf{V}} \cdot \hat{\nabla} \hat{\mathbf{V}} \right) = -\hat{\nabla} \hat{P} + \mu \left[\hat{\nabla}^2 \hat{\mathbf{V}} + \frac{1}{3} \hat{\nabla} (\hat{\nabla} \cdot \hat{\mathbf{V}}) \right] \tag{2.5}$$

where $\hat{\mathbf{V}}$ denotes the velocity vector, $\hat{P}$ denotes the pressure and μ is the kinematic viscosity. Finally, the equation of state is given by the ideal gas law:

$$\hat{P} = \hat{\rho} R^{\circ} \hat{T}. \tag{2.6}$$

To analyze the above system we will simplify matters and assume constant transport properties, i.e. constant values of c_p, λ, $\hat{\rho}\hat{\mathcal{D}}_i$, and μ.

2.1.1 Nondimensionalization

We start by nondimensionalizing all variables. The characteristic velocity is chosen to be the adiabatic flame speed, S_f°, i.e. the speed of a conservative planar flame. The length scale is chosen to be the thermal thickness $l_D = \frac{\hat{\lambda}_u}{\hat{\rho}_u c_p S_f^{\circ}}$ and the thermal time scale is $\frac{l_D}{S_f^{\circ}}$. The remaining variables are scaled with respect to their values in the fresh mixture. Upon introducing the non-dimensional variables:

$$\mathbf{V} = \frac{\hat{\mathbf{V}}}{S_f^{\circ}} \qquad \mathbf{X} = \frac{\hat{\mathbf{X}}}{l_D} \qquad T = \frac{\hat{T}}{\hat{T}_u},$$

$$\rho = \frac{\hat{\rho}}{\hat{\rho}_u} \qquad P = \frac{\hat{P}}{\hat{P}_u},$$

our system of equations takes the following form:

$$\rho \frac{DT}{Dt} - \nabla^2 T = q\Omega \tag{2.7}$$

$$\rho \frac{DY_D}{Dt} - Le_D^{-1} \nabla^2 Y_D = -\Omega \tag{2.8}$$

$$\rho \frac{DY_E}{Dt} - Le_E^{-1} \nabla^2 Y_E = -\nu\Omega \tag{2.9}$$

$$\frac{\partial \rho}{\partial t} + \nabla \cdot (\rho \mathbf{V}) = 0 \tag{2.10}$$

$$\rho\left(\frac{\partial \mathbf{V}}{\partial t}+\mathbf{V}\cdot\nabla\mathbf{V}\right)=\frac{-1}{\gamma Ma^2}\nabla P+Pr\left[\nabla^2\mathbf{V}+\frac{1}{3}\nabla(\nabla\cdot\mathbf{V})\right], \tag{2.11}$$

$$P=\rho T. \tag{2.12}$$

Parameters appearing in these equations include the Lewis numbers

$$Le_i=\frac{\hat{\lambda}}{\hat{\rho}c_p\hat{\mathcal{D}}_i},$$

which are the ratios of thermal diffusivity of the mixture to mass diffusivity of species i, the Prandtl number

$$Pr=\frac{\hat{\mu}c_p}{\hat{\lambda}},$$

which is the ratio of viscous to thermal effects and the Mach number

$$M_a=\frac{S_f^\circ}{\sqrt{\frac{\gamma\hat{P}_u}{\hat{\rho}_u}}},$$

which describes the ratio of flame speed to sound speed. Here γ is the ratio of specific heats and $\hat{P}_u$ is the characteristic pressure. Additional parameters are the heat release $q=\frac{\hat{Q}}{c_p\hat{T}_u\nu_D w_D}$ and the stoichiometric coefficient $\nu=\frac{\nu_E W_E}{\nu_D W_D}$. The reaction rate term on the right hand side of (2.8)-(2.9) has the form:

$$\Omega=D\rho^2Y_EY_De^{\frac{-E}{R\hat{T}_uT}},$$

where D is the Damköhler number, a ratio of the flow time to the chemical time, given by the following:

$$D=\frac{\hat{\lambda}_u}{c_p(S_f^\circ)^2}\frac{\nu_D B}{W_E}. \tag{2.13}$$

Of interest here are premixed flames that propagate much slower than the sound speed. Consequently, the Mach number is small and thus the pressure remains close

to its ambient value. We therefore introduce the expansion

$$P = 1 + \gamma M_a^2 p,$$

so that the momentum equation simplifies to

$$\rho\left(\frac{\partial \mathbf{V}}{\partial t} + \mathbf{V}\cdot\nabla\mathbf{V}\right) = -\nabla p + Pr\left[\nabla^2\mathbf{V} + \frac{1}{3}\nabla(\nabla\cdot\mathbf{V})\right],$$

and the equation of state takes the form

$$\rho T = 1. \tag{2.14}$$

2.1.2 Reaction Zone as a Boundary Layer

The above equations are extremely complicated for two reasons. First, the system is fully coupled. The equations of hydrodynamics couple to the transport processes because of thermal expansion of the gas. Density variations affect the velocity field through the continuity equation. The coupling in the other direction occurs through convection. Secondly, the system is highly nonlinear. In addition to the convective nonlinearities, there is the extremely nonlinear reaction rate term. The objective here is to derive from this system a reduced model of premixed flame propagation in a formal asymptotic way. We first treat the reaction rate term in a manner similar to that done by Matkowsky and Sivashinsky [7] for a single reactant model.

Both the activation energy (E) and Damkhöler number (D) are large in combustion problems. Dimensionless activation energies are typically on the order of $10 \sim 20$ while values of D can be much larger than 10^{10}. The technique of High Activation Energy Asymptotics involves rescaling D as:

$$D = \Lambda_s e^{\frac{E}{R\hat{T}_u T_a}} \tag{2.15}$$

where T_a is the adiabatic flame temperature so that with this scaling the reaction rate term takes the form:

$$\Omega = \Lambda_s \rho^2 Y_E Y_D e^{\frac{E}{RT_a}(\frac{1}{T_a} - \frac{1}{T})}. \tag{2.16}$$

In the realistic limit of large activation energy, the reaction can be readily shown to be confined to a narrow region in the flow field. Firstly, in regions of the flow where $T < T_a$, Ω is seen to be exponentially small and can thus be neglegted. In these regions, the flow is said to be frozen. Secondly, if T were to exceed T_a, then it must be true that either $Y_E = 0$ or $Y_D = 0$ to prevent an exponentially large reaction rate term. Here the flow is in equilibrium. Only where $T \approx T_a$, or more precisely where $T - T_a = O(\frac{1}{E})$ will Ω be of $O(1)$. Thus, in the limit of large activation energy, i.e. $E \gg 1$, the chemical reaction is confined to a reactive boundary layer. Within this boundary layer, gradients are steep and a balance between diffusion and reaction is maintained. In the outer regions on either side of the reaction sheet, reaction is negligible and convection balances diffusion. The method of matched asymptotics is employed to analyze each region separately and the matching procedure results in jump conditions relating the solutions in the outer regions across the reaction zone.

In this study, we assume near unity Lewis numbers and near-stoichiometric conditions so that the following expansions are introduced

$$Le_i = 1 + \frac{\epsilon l_i}{q} \qquad\qquad \hat{\phi} = 1 + \epsilon \hat{\phi}_1,$$

where ϵ is a small dimensionless parameter, inversely proportional to E, and is defined shortly. It is also assumed that temperature gradients behind the flame are small. In analyses such as this, it is convenient to work with the enthalpy functions (or Shvab-Zel'dovich variables) given by

$$H_D = T + qY_D \qquad\qquad H_E = T + \frac{q}{\nu} Y_E. \tag{2.17}$$

The advantage of working with H_i is that their governing equations, obtained by appropriately summing (2.8) and (2.9) with (2.7) are free of the nonlinear reaction rate term. In particular these equations are

$$\rho\frac{\partial H_D}{\partial t} + \rho\mathbf{V}\cdot\nabla H_D - \nabla^2 H_D = -\frac{\epsilon l_D}{q}\nabla^2(H_D - T)$$

$$\rho\frac{\partial H_E}{\partial t} + \rho\mathbf{V}\cdot\nabla H_E - \nabla^2 H_E = -\frac{\epsilon l_E}{q}\nabla^2(H_E - T),$$

which is used in place of those of Y_i. Note that once T and H are determined, the species concentration can easily be determined using the above definitions for H. As mentioned earlier, temperature gradients are assumed small, i.e. $O(\epsilon)$, behind the flame. In addition, only an $O(\epsilon)$ amount of species leak through and therefore, the enthalpy variables can be expanded as

$$H_D = T_a + \epsilon h_D \qquad\qquad H_E = T_a + \epsilon h_E,$$

where T_a is the adiabatic flame temperature. The equations for the enthalpy perturbations, h_i, are

$$\rho\frac{\partial h_D}{\partial t} + \rho\mathbf{V}\cdot\nabla h_D - \nabla^2 h_D = -\frac{l_D}{q}\nabla^2 T \tag{2.18}$$

$$\rho\frac{\partial h_E}{\partial t} + \rho\mathbf{V}\cdot\nabla h_E - \nabla^2 h_E = -\frac{l_E}{q}\nabla^2 T. \tag{2.19}$$

2.1.3 Planar Flame

The steady, one-dimensional form of the system of equations (2.7)- (2.10) can be analyzed in the limit $E \gg 1$ to provide a description of a planar adiabatic flame, c.f. [9] and [15]. Here, a summary of some of the essential results is given. A uniform flow, $u = 1$, is supplied at $x = -\infty$, and only the transport equations need to be

treated. In particular, steady state profiles for T, Y_i in the outer flow on either side of the reaction zone are found to be

$$T = \begin{cases} 1 + qY_{D,-\infty}e^x + O(\epsilon) & x < 0 \\ T_a & x > 0. \end{cases}$$

$$Y_D = \begin{cases} Y_{D,-\infty}(1 - e^x) + O(\epsilon) & x < 0 \\ 0 & x > 0. \end{cases}$$

$$Y_E = \begin{cases} Y_{E,-\infty}(1 - e^x) + O(\epsilon) & x < 0 \\ \epsilon Y_{D,-\infty}\hat{\phi}_1 & x > 0. \end{cases}$$

where solutions have been sought in power series in ϵ, i.e.

$$T = T^0 + \epsilon T^1 + \cdots \qquad Y_i = Y_i^0 + \epsilon Y_i^1 + \cdots.$$

Note that for the planar flame, the deficient reactant is always consumed behind the flame. It remains to determine the adiabatic flame speed, S_f°, which appears in Λ_s. This information is obtained by analyzing the reaction zone where we introduce the stretched variable, $x = \epsilon\xi$, and the expressions

$$T = T_a + \epsilon\theta + ... \qquad Y_D = \epsilon Z_D \qquad Y_E = \epsilon Z_E.$$

The local enthalpy variables

$$h_D = \theta + qZ_D \qquad h_E = \theta + qZ_E,$$

are found to remain constant throughout the reaction zone and matching to the burned side determines these constants to be

$$h_D = 0 \qquad h_E = qY_{D,-\infty}\hat{\phi}_1.$$

The leading-order local equation for the perturbed temperature is then found to be

$$\frac{d^2\theta}{d\xi^2} = \Lambda_s'\theta(qY_{D,-\infty}\hat{\phi}_1 - \theta)e^{\theta}, \tag{2.20}$$

where $\Lambda_s' = \frac{\Lambda_s\epsilon^3}{q(T_a)^2}$ and we have defined $\epsilon = \frac{R\hat{T}_u T_a^2}{E}$. This equation has a first integral of the form

$$\frac{1}{2}\theta_\xi^2 = \Lambda_s'\left(qY_{D,-\infty}\hat{\phi}_1(\theta e^{\theta} - e^{\theta}) - \theta^2 e^{\theta} + 2(\theta e^{\theta} - e^{\theta})\right) + \text{constant}.$$

Matching to the burned side where $\theta \sim 0$ determines the constant to be

$$\text{constant} = \Lambda_s'(2 + qY_{D,-\infty}).$$

Finally, matching to the unburned side where $\theta \sim \xi qY_{D,-\infty}$ yields an expression for the burning rate eigenvalue, Λ_s', namely

$$\Lambda_s' = \frac{Q^2}{2(2+\phi)}, \tag{2.21}$$

where $Q = qY_{D,-\infty}$ and $\phi = qY_{D,-\infty}\hat{\phi}_1$. Using (2.21) and (2.13) we obtain an expression for the flame speed

$$S_f^\circ = \left(\frac{\hat{\lambda}_u\nu\nu_D B}{qc_p W_E T_a^2}\frac{2(2+\phi)\epsilon^3}{Q^2}\right)^{\frac{1}{2}} e^{\frac{-1}{2\epsilon T_a}} \tag{2.22}$$

where $T_a = 1+Q$ is the adiabatic flame temperature. This expression for flame speed has been shown to achieve a maximum value slightly on the rich side of stoichiometry, consistent with experimental measurements [9], [15].

2.1.4 Analysis of Reaction Zone for a Multi-dimensional Flame.

The analysis of the preceding sub-section can be generalized for flames of arbitrary shape. We again only treat the transport equations, and upon using the expression

for Λ_s our equations become

$$\rho\frac{DT}{Dt} - \nabla^2 T = \frac{Q^2 q^2}{2(2+\phi)\epsilon^3}\rho^2 Y_E Y_D e^{\frac{E}{R\hat{T}_u}(\frac{1}{T_a}-\frac{1}{T})} \tag{2.23}$$

$$\rho\frac{DY_D}{Dt} - Le_D^{-1}\nabla^2 Y_D = \frac{-Q^2 q}{2(2+\phi)\epsilon^3}\rho^2 Y_E Y_D e^{\frac{E}{R\hat{T}_u}(\frac{1}{T_a}-\frac{1}{T})} \tag{2.24}$$

$$\rho\frac{DY_E}{Dt} - Le_E^{-1}\nabla^2 Y_E = -\nu\frac{Q^2 q}{2(2+\phi)\epsilon^3}\rho^2 Y_E Y_D e^{\frac{E}{R\hat{T}_u}(\frac{1}{T_a}-\frac{1}{T})} \tag{2.25}$$

In the limit that $\epsilon \to 0$ the reaction rate term is only important in the narrow reaction diffusion layer. Outside of this boundary layer, solutions are sought in the form of power series in ϵ, i.e.

$$T^{out} = T^0 + \epsilon T^1 + \cdots \qquad \rho = \rho^0 + \epsilon\rho^1 + \cdots$$

$$H_D^{out} = 1 + qY_{D,-\infty} + \epsilon h_D + \cdots \qquad H_E^{out} = 1 + \frac{q}{\nu}Y_{E,-\infty} + \epsilon h_E + \cdots.$$

Upon substituting into the expressions, (2.17) and (2.18), we get the following enthalpy equations on either side of the reaction zone:

$$\rho^0\left[\frac{\partial h_D}{\partial t} + \mathbf{V}\cdot\nabla h_D\right] - \nabla^2 h_D = \frac{l_D}{q}\nabla^2 T^0, \quad x \neq f \tag{2.26}$$

$$\rho^0\left[\frac{\partial h_E}{\partial t} + \mathbf{V}\cdot\nabla h_E\right] - \nabla^2 h_E = \frac{l_E}{q}\nabla^2 T^0, \quad x \neq f. \tag{2.27}$$

From (2.23) the $O(1)$ temperature is determined from

$$\rho^0\left(\frac{\partial T^0}{\partial t} + \mathbf{V}\cdot\nabla T^0\right) - \nabla^2 T^0 = 0, \quad x < f \tag{2.28}$$

$$T^0 = 1 + qY_{D,-\infty}, \quad x > f. \tag{2.29}$$

By definition, h_i are directly related to the temperature perturbations, T_1, and thus we retain the appropriate equations from (2.23), (2.14), i.e.

$$\rho^1\left(\frac{\partial T^0}{\partial t}+V\cdot\nabla T^0\right)+\rho^0\left(\frac{\partial T^1}{\partial t}+V\cdot\nabla T^1\right)-\nabla^2T^1=0,\quad x\neq f,$$

$$\rho^0T^0=1,\qquad\qquad \rho^1=\frac{-T^1}{(T^0)^2}. \tag{2.30}$$

An analysis of the reaction zone is needed to relate the outer variables on either side. We first adopt a coordinate system attached to the front

$$\xi=x-f(y,z,t)\qquad y=y\qquad z=z\qquad t=t,$$

such that

$$\frac{\partial}{\partial x}\to\frac{\partial}{\partial\xi}\qquad\qquad \frac{\partial}{\partial y}\to\frac{\partial}{\partial y}-f_y\frac{\partial}{\partial\xi}$$
$$\frac{\partial}{\partial z}\to\frac{\partial}{\partial z}-f_z\frac{\partial}{\partial\xi}\qquad\qquad \frac{\partial}{\partial t}\to\frac{\partial}{\partial t}-f_t\frac{\partial}{\partial\xi},$$

and the Laplacian operator takes the following form

$$\nabla^2=(1+f_y^2+f_z^2)\frac{\partial^2}{\partial\xi^2}+\frac{\partial^2}{\partial y^2}+\frac{\partial^2}{\partial z^2}-(f_{yy}+f_{zz})\frac{\partial}{\partial\xi}-2f_y\frac{\partial^2}{\partial\xi\partial y}-2f_z\frac{\partial^2}{\partial\xi\partial z}. \tag{2.31}$$

To examine the structure of the inner layer we introduce a stretched variable $\xi=\epsilon\zeta$ and then seek solutions of the form:

$$T=T_a+\epsilon\theta+\cdots\qquad H_D=T_a+\epsilon\Psi+\cdots\qquad H_E=T_a+\epsilon\chi+\cdots.$$

These expansions are substituted into (2.18), (2.19) and (2.23) to obtain a system of equations for the local temperature and species profiles. The appropriate leading order equations are

$$\frac{\partial^2\Psi}{\partial\xi^2}=0 \tag{2.32}$$

$$\frac{\partial^2 \chi}{\partial \xi^2} = 0 \tag{2.33}$$

$$-(1 + f_y^2 + f_z^2)\frac{\partial^2 \theta}{\partial \xi} = \frac{Q^2}{2(2+\phi)}(\chi - \theta)(\Psi - \theta)e^{\theta}. \tag{2.34}$$

Solutions to these equations should match to the outer solutions (2.26)-(2.29). The matching conditions can be derived by expanding the outer solutions in terms of the inner variable $\xi = \epsilon\zeta$, to obtain

$$T^{out}(\xi = \epsilon\zeta) \sim T^0(0\pm) + \epsilon\left[T^1(0\pm) + \zeta\frac{\partial T^0}{\partial \xi}(0\pm)\right] + \cdots. \tag{2.35}$$

Similarly, the appropriate expressions for species are

$$Y_i^{out}(\xi = \epsilon\zeta) \sim Y_i^0(0\pm) + \epsilon\left[Y_i^1(0\pm) + \zeta\frac{\partial Y_i^0}{\partial \xi}(0\pm)\right] + \cdots. \tag{2.36}$$

However, we need conditions for the reduced enthalpy variables, which follow from the definition (2.17) and using the fact that $Y_i^0(0+) = 0$. The resulting conditions are

$$1 + Q + \epsilon h_D(0+) = T^0(0+) + \epsilon\left[T^1(0+) + qY_D^1(0+)\right], \tag{2.37}$$

and

$$1 + \frac{q}{\nu}Y_{E,-\infty} + \epsilon h_E(0+) = T^0(0+) + \epsilon\left[T^1(0+) + \frac{q}{\nu}Y_E^1(0+)\right]. \tag{2.38}$$

From (2.37) it follows that

$$T_a = 1 + Q, \tag{2.39}$$

$$h_D(0+) = T^1(0+) + qY_D^1(0+). \tag{2.40}$$

Similarly, from (2.38) after using the expansion for $\hat{\phi}$ we get

$$h_E(0+) = T^1(0+) + \frac{q}{\nu} Y_E^1(0+) - \phi. \tag{2.41}$$

Upon solving (2.32) and (2.33), we find χ and Ψ are constant throughout the reaction zone. Matching to the burned side determines that

$$\chi = T^1(0+) + \frac{q}{\nu} Y_E^1(0+), \tag{2.42}$$

and

$$\Psi = T^1(0+) + q Y_D^1(0+). \tag{2.43}$$

The equation for the local temperature distribution (2.34) can now be easily integrated. Upon multiplying through by $\frac{\partial \theta}{\partial \xi}$ we obtain the first integral

$$\begin{aligned} -(1 + f_y^2 + f_z^2) \left(\frac{\partial \theta}{\partial \xi} \right)^2 &= 2\Lambda_s \left(\chi \Psi e^\theta - \chi(\theta e^\theta - e^\theta) - \Psi(\theta e^\theta - e^\theta) + \theta^2 e^\theta \right) \\ &\quad + 2\Lambda_s \left(-2(\theta e^\theta - e^\theta) \right) + \text{constant}. \end{aligned} \tag{2.44}$$

Matching to the burned side, $\xi \to \infty$, where $\frac{\partial T^0}{\partial \xi}(0+) = 0$, yields

$$\text{constant} = \Lambda_s e^{T_b^1} \left(\chi \Psi - (\chi + \Psi)(T_b^1 - 1) + (T_b^1)^2 - 2T_b^1 + 2 \right), \tag{2.45}$$

where $T_b^1 = T^1(0+)$. Matching now to $\xi \to -\infty$, i.e. the unburned side, yields the condition for the outer temperature gradient

$$\sqrt{1 + f_y^2 + f_z^2} \, \frac{\partial T^0}{\partial \xi}(0-) = \sqrt{2\Lambda_s} e^{T_b^1} \sqrt{\chi \Psi - (\chi + \Psi)(T_b^1 - 1) + (T_b^1)^2 - 2T_b^1 + 2}. \tag{2.46}$$

We note that one or the other species must vanish behind the flame and thus $Y_E^1(0+)\, Y_D^1(0+) \equiv 0$. Using this fact, when the expression for χ, Ψ, (2.42), (2.43) are

inserted, condition (2.46) simplifies to

$$\sqrt{1+f_y^2+f_z^2}\,\frac{\partial T^0}{\partial \xi}(0-) = \sqrt{2\Lambda_s}\,\sqrt{2+q(Y_D^1+\frac{1}{\nu}Y_E^1)}\,e^{T_b^1},$$

which we can write as

$$\sqrt{1+f_y^2+f_z^2}\,\frac{\partial T^0}{\partial \xi}(0-) = \sqrt{2\Lambda_s}\,\sqrt{2+qY_{LE}}\,e^{T_b^1},$$

where Y_{LE} denotes the locally excess reactant. Recall that, for the planar flame, the initially deficient reactant is always consumed at the flame, i.e. $Y_D(0+)=0$ and thus $Y_{LE}=\frac{Y_E(0+)}{\nu}$. For a curved flame in non-uniform flow fields, however, it is possible, due to disparate diffusivities, for the initially excess species to be locally deficient, and hence, consumed by the reaction. In this case, a small amount of the initially deficient reactant leaks through, and $Y_{LE}=Y_D(0+)$.

This final condition on the temperature gradient depends on the temperature perturbation behind the flame and the amount of locally excess reactant that leaks through the flame. Both of these quantities can be expressed in terms of the enthalpy perturbations behind the flame.

To determine which species is consumed and which leaks through, we re-consider (2.40) and (2.41). Subtracting one from the other gives

$$\frac{q}{\nu}Y_E^1(0+) - qY_D^1(0+) = \phi + h_E(0+) - h_D(0+). \tag{2.47}$$

The sign of the right hand side of (2.47) now provides the necessary information. If the right hand side is positive, then $Y_D^1=0$ and (2.47) determines the amount of excess reactant that leaks through. Equation (2.38) then determines the flame temperature perturbation to be $T_b^1=h_D(0+)$. When these are inserted into (2.44) our final jump condition becomes

$$\sqrt{1+f_y^2+f_z^2}\,\frac{\partial T^0}{\partial \xi}(0-) = -Q\sqrt{\frac{2+\phi+h_E(0+)-h_D(0+)}{2+\phi}}\,e^{\frac{h_D(0+)}{2}}. \tag{2.48}$$

On the other hand, if the right hand side of (2.47) is negative, then $Y_E^1(0+) = 0$ and (2.47) determines the amount of deficient reactant that leaks through. Equation (2.41) then determines the flame temperature perturbation to be $T_b^1 = h_E(0+) + \phi$. When these are inserted into (2.46), our final jump condition becomes

$$\sqrt{1+f_y^2+f_z^2}\,\frac{\partial T^0}{\partial \xi}(0-) = -Q\sqrt{\frac{2-\phi+h_D(0+)-h_E(0+)}{2+\phi}}\,e^{\frac{h_E(0+)+\phi}{2}}. \tag{2.49}$$

To summarize our jump conditions relating the outer variables across the front, we first note that matching has shown that T^0, h_D^0, h_E^0 are all continuous across the flame sheet. Furthermore, direct integration of the reaction-free equations (2.26)-(2.27) across the flame yield the jump relations

$$\left[\frac{\partial h_D}{\partial \xi}\right]_{\xi=0} + \frac{l_D}{q}\left[\frac{\partial T^0}{\partial \xi}\right]_{\xi=0} = 0. \tag{2.50}$$

$$\left[\frac{\partial h_E}{\partial \xi}\right]_{\xi=0} + \frac{l_E}{q}\left[\frac{\partial T^0}{\partial \xi}\right]_{\xi=0} = 0, \tag{2.51}$$

where the jump [ ] denotes burned minus unburned quantities. The final jump condition is either (2.48) or (2.49) depending on the sign of $\phi + h_E(0+) - h_D(0+)$.

The problem has now been reduced to solving the transport equations (2.7)-(2.9) subject to the jump conditions (2.50) and (2.51) and the appropriate jump in the temperature gradient given either by (2.48), if $Y_D^1(0+) = 0$ or (2.49), if $Y_E^1(0+) = 0$. These results can now be generalized by recognizing that the normal derivative is given by:

$$\frac{\partial}{\partial \mathbf{n}} = \mathbf{n}\cdot\nabla = \sqrt{1+f_y^2+f_z^2}\,\frac{\partial}{\partial \xi} - \left(\sqrt{1+f_y^2+f_z^2}\right)^{-1}\left(f_y\frac{\partial}{\partial y} + f_z\frac{\partial}{\partial z}\right). \tag{2.52}$$

Since there are no jumps in the transverse, y and z, directions it follows that

$$\left[\frac{\partial}{\partial \mathbf{n}}\right] = \sqrt{1+f_y^2+f_z^2}\left[\frac{\partial}{\partial \xi}\right].$$

The jump conditions can now be written in a generalized coordinate-free form:

$$\left[T^0\right] = 0 \qquad [h_D] = 0 \qquad [h_E] = 0 \tag{2.53}$$

$$\left[\frac{\partial h_D}{\partial \mathbf{n}}\right] + \frac{l_D}{q}\left[\frac{\partial T^0}{\partial \mathbf{n}}\right] = 0 \tag{2.54}$$

$$\left[\frac{\partial h_E}{\partial \mathbf{n}}\right] + \frac{l_E}{q}\left[\frac{\partial T^0}{\partial \mathbf{n}}\right] = 0 \tag{2.55}$$

and

$$\left[\frac{\partial T^0}{\partial \mathbf{n}}\right] = -Q\sqrt{\frac{2+\phi+h_E-h_D}{2+\phi}}\, e^{\frac{h_D(0+)}{2}}, \qquad \text{if } \phi + h_E - h_D > 0, \tag{2.56a}$$

$$\left[\frac{\partial T^0}{\partial \mathbf{n}}\right] = -Q\sqrt{\frac{2-\phi+h_D-h_E}{2+\phi}}\, e^{\frac{h_E(0+)+\phi}{2}}, \qquad \text{if } \phi + h_E - h_D < 0. \tag{2.56b}$$

The local analysis of the reaction zone has effectively replaced the nonlinear reaction rate term by jump relations. In particular, the variables are continuous while their gradients suffer jump discontinuities. For this reason models of this type have often been referred to as delta-function models.

2.1.5 The constant density approximation

Although we have succeeded in simplifying the nonlinear reaction rate terms appearing in the original governing equations, solutions of the resulting model are still difficult to obtain due to the coupling of the hydrodynamic and transport processes. It is possible to decouple the equations of hydrodynamics by considering weak thermal expansion. This is a rather crude approximation from a physical standpoint, but it has proven to be a useful approach to gain qualitative insights into premixed flame propagation. In this way, we can study the effect of the flow field on the flame, but

the effect of the flame on the flow field is suppressed. Assuming that density changes across the flame are small, $Q = qY_{D,-\infty} \ll 1$, we expand the transport variables as:

$$T^0 = 1 + Q\tau + ... \qquad \rho^0 = 1 + QR + ... \qquad h_D = H_D \qquad h_E = H_E.$$

Once these are inserted into our model we obtain the following generalized two reactant model:

$$\left(\frac{\partial \tau}{\partial t} + \mathbf{V}\cdot\nabla\tau\right) - \nabla^2\tau = 0, \quad \text{unburned}$$

$$\tau = 1, \quad \text{burned} \tag{2.57}$$

$$\left(\frac{\partial h_D}{\partial t} + \mathbf{V}\cdot\nabla h_D\right) - \nabla^2 h_D = l_d\nabla^2\tau, \quad x \neq f \tag{2.58}$$

$$\left(\frac{\partial h_E}{\partial t} + \mathbf{V}\cdot\nabla h_E\right) - \nabla^2 h_E = l_e\nabla^2\tau, \quad x \neq f \tag{2.59}$$

where $l_e = l_E Y_{D,-\infty}$ and $l_d = l_D Y_{D,-\infty}$. These equations are to be solved subject to the jump conditions at the flame surface $x = f$.

$$[\tau] = 0 \qquad [h_D] = 0 \qquad [h_E] = 0, \tag{2.60}$$

$$\left[\frac{\partial h_D}{\partial \mathbf{n}}\right] + l_d\left[\frac{\partial \tau}{\partial \mathbf{n}}\right] = 0, \tag{2.61}$$

$$\left[\frac{\partial h_E}{\partial \mathbf{n}}\right] + l_e\left[\frac{\partial \tau}{\partial \mathbf{n}}\right] = 0, \tag{2.62}$$

and

$$\left[\frac{\partial \tau}{\partial \mathbf{n}}\right] = \sqrt{\frac{2+\phi_1+h_E-h_D}{2+\phi_1}}\, e^{\frac{h_D(0+)}{2}}, \qquad \text{if } \phi_1 + h_E - h_D > 0, \tag{2.63a}$$

$$\left[\frac{\partial \tau}{\partial \mathbf{n}}\right] = \sqrt{\frac{2-\phi_1+h_D-h_E}{2+\phi_1}}\, e^{\frac{h_E(0+)+\phi_1}{2}}, \qquad \text{if } \phi_1 + h_E - h_D < 0, \tag{2.63b}$$

where $\phi_1 = Q\phi$. The boundary conditions are

$$\tau(-\infty) = 0 \qquad h_D(-\infty) = 0 \qquad h_E(-\infty) = 0$$

$$\tau(+\infty) = 1 \qquad h_D(+\infty) \text{ bounded} \qquad h_E(+\infty) \text{ bounded.} \tag{2.64}$$

The above system is decoupled from the equation for the temperature perturbation T_1. Also, the constant density approximation has decoupled the equations of hydrodynamics. In this model, the flow field is prescribed, allowing us to study the effect of the flow on the flame but ignoring the effect of the flame on the flow.

CHAPTER 3

DYNAMICS OF PLANAR AND STRAINED FLAMES

The model derived in the previous chapter is valid for flames of arbitrary shapes in general flow fields. In this chapter we will use it to study the behavior of planar and strained flames.

3.1 Diffusional-Thermal Instability of Planar Flames

Firstly note that for off-stoichiometric mixtures, $\Phi_1 \to \infty$, it is clear that

$$\phi_1 + h_E - h_D > 0$$

and thus the first jump relation, (2.63a) for the temperature gradient is appropriate. We observe that this condition reduces to

$$\left[\frac{\partial \tau}{\partial \mathbf{n}}\right] = -e^{\frac{h_D(0+)}{2}}$$

which is identical to that derived in the single-reactant theory. Thus our model appropriately describes the flame behavior in conditions far removed from stoichiometry. When conditions are closer to stoichiometry, both species will play a role in flame dynamics.

The linear stability of a planar flame in a near-stoichiometric mixture has been studied previously by Joulin and Mitani, [11], and their results are readily obtained by linearizing our model. In particular, it is easy to show that $h_E(0+) = h_D(0+) = 0$ for the planar flame and thus the first jump relation is again the appropriate one to use.

Consider a planar flame in a uniform flow field with the prescribed flow field $\mathbf{V} = (1, 0, 0)$ located at $x = 0$. A steady one-dimensional solution to our system

subject to the jump conditions given by (2.60) -(2.63b) is

$$\tau^s = \begin{cases} e^x & x < 0 \\ 1 & x > 0, \end{cases} \tag{3.1}$$

$$h_D^s = \begin{cases} -l_d x e^x & x < 0 \\ 0 & x > 0, \end{cases} \tag{3.2}$$

$$h_E^s = \begin{cases} -l_e x e^x & x < 0 \\ 0 & x > 0. \end{cases} \tag{3.3}$$

We impose small arbitrary disturbances on these solutions of the form

$$\tau = \tau^s + \delta T(x,y,t) \qquad h_D = h_D^s + \delta H_D(x,y,t) \qquad h_E = h_E^s + \delta H_E(x,y,t),$$

where δ is a small amplitude. The perturbed front location is $x = \delta \hat{A} e^{\omega t} e^{iKy}$, where $\hat{A}$ is the amplitude of the perturbed front. These expressions are inserted into our system and the resulting system is linearized. Solutions of the perturbed quantities are sought in the form

$$T(x,y,t) = \hat{T} e^{\omega t} e^{iKy} \quad H_D(x,y,t) = \hat{H}_D e^{\omega t} e^{iKy} \qquad H_E = \hat{H}_E e^{\omega t} e^{iKy},$$

which yields the following system

$$\frac{\partial^2 \hat{T}}{\partial x^2} - \frac{\partial \hat{T}}{\partial x} - (\omega + K^2)\hat{T} = 0, \quad x < f \tag{3.4}$$

$$\hat{T} = 0, \quad x > f \tag{3.5}$$

$$\frac{\partial^2 \hat{H}_D}{\partial x^2} - \frac{\partial \hat{H}_D}{\partial x} - (\omega + K^2)\hat{H}_D = l_d(K^2 \hat{T} - \frac{\partial^2 \hat{T}}{\partial x^2}), \quad x \neq f \tag{3.6}$$

$$\frac{\partial^2 \hat{H}_E}{\partial x^2} - \frac{\partial \hat{H}_E}{\partial x} - (\omega + K^2)\hat{H}_E = l_e(K^2\hat{T} - \frac{\partial^2 \hat{T}}{\partial x^2}), \quad x \neq f \tag{3.7}$$

to be solved subject to the following jump conditions evaluated at the unperturbed location $x = 0$

$$\left[\hat{T}\right] = \hat{A} \qquad \left[\hat{H}_D\right] = -\hat{A}l_d \qquad \left[\hat{H}_E\right] = -\hat{A}l_e \tag{3.8}$$

$$\left[\frac{\partial \hat{h}_D}{\partial x}\right]_{x=0} + l_d \left[\frac{\partial \hat{T}}{\partial x}\right]_{x=0} = -\hat{A}l_d \tag{3.9}$$

$$\left[\frac{\partial \hat{h}_E}{\partial x}\right]_{x=0} + l_e \left[\frac{\partial \hat{T}}{\partial x}\right]_{x=0} = -\hat{A}l_e \tag{3.10}$$

$$\left[\frac{\partial \hat{T}}{\partial x}\right]_{x=0} = \frac{-\hat{A}}{2(2+\phi_1)}\left[\hat{H}_E(0+) + \hat{H}_D(0+)(1+\phi_1)\right]. \tag{3.11}$$

The solution of the above system with $Re(\omega) > 0$ is given by:

$$\hat{T} = \begin{cases} -\hat{A}e^{m_+ x} & x < 0 \\ 0 & x > 0. \end{cases} \tag{3.12}$$

$$\hat{h}_D = \begin{cases} \frac{-\hat{A}l_d(m_+^2 - K^2)}{(m_+ - m_-)^2}e^{m_+ x} + \frac{\hat{A}l_d}{m_+ - m_-}e^{m_+ x} + \hat{A}l_d e^{m_+ x} + \\ \frac{\hat{A}l_d(m_+^2 - K^2)}{m_+ - m_-}xe^{m_+ x} & x < 0 \\ \frac{-\hat{A}l_d(m_+^2 - K^2)}{(m_+ - m_-)^2}e^{m_- x} + \frac{\hat{A}l_d}{m_+ - m_-}e^{m_- x} & x > 0, \end{cases} \tag{3.13}$$

$$\hat{h}_E = \begin{cases} \frac{-\hat{A}l_e(m_+^2-K^2)}{(m_+-m_-)^2}e^{m_+x} + \frac{\hat{A}l_e}{m_+-m_-}e^{m_+x} + \hat{A}l_e e^{m_+x} + & \\ \frac{\hat{A}l_e(m_+^2-K^2)}{m_+-m_-}xe^{m_+x} & x<0 \\ \frac{-\hat{A}l_e(m_+^2-K^2)}{(m_+-m_-)^2}e^{m_-x} + \frac{\hat{A}l_e}{m_+-m_-}e^{m_-x} & x>0. \end{cases} \tag{3.14}$$

where m_+ and m_- are given by:

$$m_+ = \frac{1}{2} + \sqrt{1+4(\omega+K^2)} \quad m_- = \frac{1}{2} - \sqrt{1+4(\omega+K^2)}$$

such that $Re(m_+ > 0)$ and $Re(m_- < 0)$. In order that nontrivial solutions exist, we find ω must satisfy the cubic equation:

$$\begin{aligned} 64\omega^3 + \omega^2(192K^2+32+16L-4L^2) &+ 4\omega(12K^2+1)(4K^2+L+1) \\ &+ 4K^2(4K^2+L+1)^2 = 0, \end{aligned} \tag{3.15}$$

where L is a lumped Lewis number given by $L = \frac{l_e+l_d+l_d\phi_1}{4+2\phi_1}$. This is identical to the result of the single reactant theory with L appearing in the place of l_d. The neutral stability boundaries of the above dispersion relation, shown in figure 3.1, determine a range of Lewis number $-1 < L < 2(1+\sqrt{3})$ for which planar flames are stable to disturbances of all wavelength. The left boundary is given by $L = -1 - 4K^2$, and it is referred to as the cellular boundary because $Im(\omega) = 0$ as well. As L is decreased below -1 the plane flame will lose stability to a stationary cellular structure. Along the right stability, $Im(\omega) \neq 0$, and thus the planar flame will lose stability to pulsations or travelling waves.

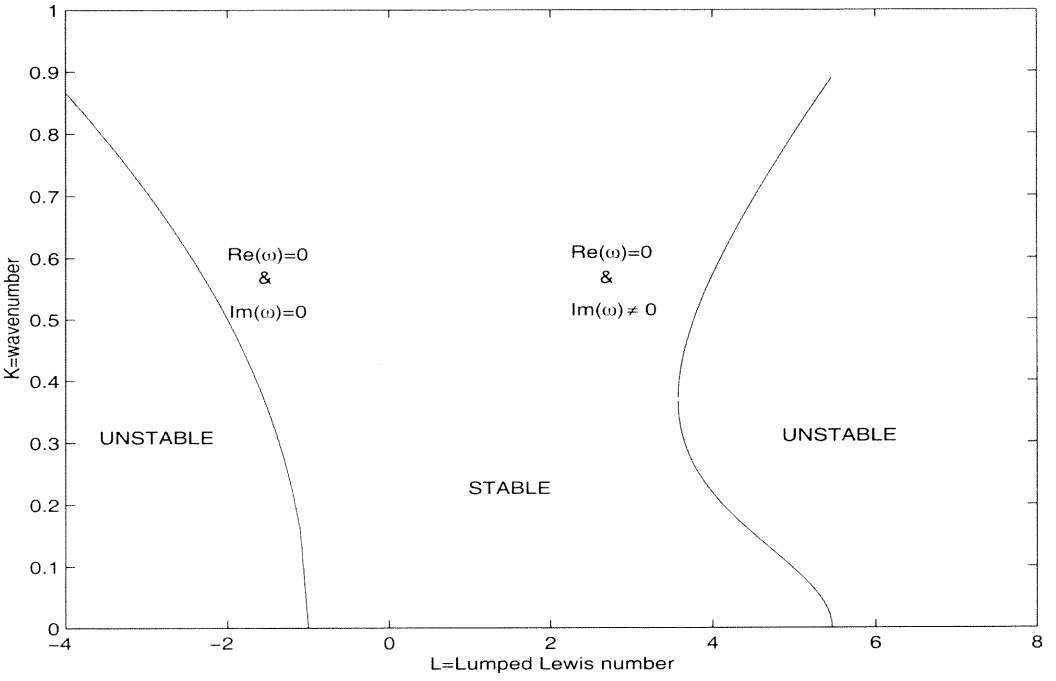

Figure 3.1: Neutral Stability Curves

3.2 Extinction of Near-Stoichiometric flames in Stagnation Point Flow

As demonstrated in the previous section, for the planar flame, there is no temperature perturbation in the burned region, i.e. $h_E(0+) = h_D(0+) = 0$, and thus the initially deficient reactant remains deficient everywhere. Consequently, $\phi_1 + h_E - h_D > 0$ and the first condition in (2.63a) is always used to determine the jump in the temperature gradient.

However, it is known that curvature and aerodynamic straining can induce temperature perturbations behind the flame. When the two species diffuse at unequal rates, i.e. different Lewis numbers, it is possible that one or the other jump conditions (2.63a) or (2.63b) is needed.

Here we consider a positively stretched flame in a stagnation point flow. As shown in figure 3.2 the flow originates at $x = -\infty$ and impinges against a wall located at $x = 0$. This configuration supports a planar flame situated at $x = -d$.

The flow remains potential flow in the absense of density variations and is given by $\mathbf{V} = k(-x, y)$.

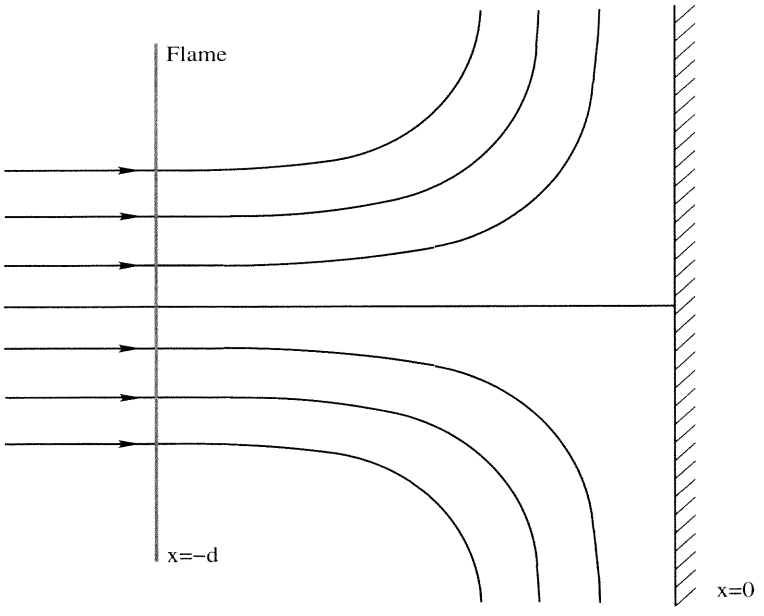

Figure 3.2: Flame in stagnation point flow

We seek steady solutions with no variations in the y direction so that our governing equations become

$$-kxT_x = T_{xx}, \quad x < -d \tag{3.16}$$

$$T = 1, \quad x > -d \tag{3.17}$$

$$-kxh_x^D = h_{xx}^D + l_d T_{xx}, \quad x \neq -d \tag{3.18}$$

$$-kxh_x^E = h_{xx}^E + l_e T_{xx}, \quad x \neq -d. \tag{3.19}$$

These equations are to be solved subject to the following jump conditions which are all evaluated at $x = -d$:

$$[T] = 0, \qquad [h_i] = 0, \tag{3.20}$$

$$\left[\frac{\partial h_i}{\partial x}\right] + l_i \left[\frac{\partial T}{\partial x}\right] = 0, \tag{3.21}$$

$$\left[\frac{\partial T}{\partial x}\right] = \sqrt{1 + \frac{1}{2A}(h_E - h_D)}\, e^{\frac{h_D(0+)}{2}}, \qquad \text{if } \phi_1 + h_E - h_D > 0, \tag{3.22a}$$

$$\left[\frac{\partial T}{\partial x}\right] = \sqrt{\varphi - \frac{1}{2A}(h_E - h_D)}\, e^{\frac{h_E(0+)+\phi_1}{2}}, \qquad \text{if } \phi_1 + h_E - h_D < 0. \tag{3.22b}$$

where $\varphi = \frac{2-\phi_1}{2+\phi_1}$. The boundary conditions are

$$T(-\infty) = 0, \qquad h_D(-\infty) = 0, \qquad h_E(-\infty) = 0$$

$$\frac{dh_D}{dx}(0-) = 0, \qquad \frac{dh_E}{dx}(0-) = 0 \tag{3.23}$$

We begin by integrating (3.16) to find

$$T = C_1 \operatorname{erfc}\left(-\sqrt{\frac{k}{2}}x\right) + C_2, \tag{3.24}$$

where the complimentary error function is defined as

$$\operatorname{erfc}(z) = \int_{-\infty}^{z} e^{-\xi^2} d\xi \tag{3.25}$$

The constants of integration C_1 and C_2 can be obtained by applying the boundary condition, (3.23), and the jump condition, (3.20), which yield the solution

$$T = \begin{cases} \frac{1}{\operatorname{erfc}(\sqrt{\frac{k}{2}}d)} \operatorname{erfc}(-\sqrt{\frac{k}{2}}x) & x < 0 \\ 1 & x > 0. \end{cases} \tag{3.26}$$

We can now solve for the enthalpy variables, h_i. First, behind the flame, $-d < x < 0$, the only solution satisfying the flux condition at the wall is a constant so that $h^i = D_3^i$.

In the unburned region, $x < -d$ the appropriate governing equations are

$$h^i_{xx} + kxh^i_x = \frac{l_i k\sqrt{\frac{2k}{\pi}}}{\operatorname{erfc}\sqrt{\frac{k}{2}}d)} x\, e^{\frac{-kx^2}{2}}, \quad x < -d.$$

Multiplying both sides by $e^{\frac{kx^2}{2}}$ and integrating once we get:

$$h^i_x e^{\frac{kx^2}{2}} = \frac{l_i k\sqrt{\frac{2k}{\pi}}}{\operatorname{erfc}(\sqrt{\frac{k}{2}}d)} \frac{x^2}{2} + \hat{D}^i_1, \quad x < -d.$$

Integrating once more we get the following expression for h^i

$$h^i = \hat{D}^i_1\sqrt{\frac{\pi}{2k}}\ \operatorname{erfc}(-\sqrt{\frac{k}{2}}x) + \frac{l_i k\sqrt{\frac{2k}{\pi}}}{2\ \operatorname{erfc}(\sqrt{\frac{k}{2}}d)} \int_{-\infty}^{x} \eta^2 e^{\frac{-k\eta^2}{2}} d\eta + D^i_2, \quad x < -d$$

so that

$$h^i = \begin{cases} D^i_1\ \operatorname{erfc}(-\sqrt{\frac{k}{2}}x) - \frac{l_i\sqrt{\frac{k}{2\pi}}}{\operatorname{erfc}(\sqrt{\frac{k}{2}}d)} x\, e^{\frac{-kx^2}{2}} + D^i_2 & x < -d \\ \\ D^i_3 & -d < x < 0. \end{cases}$$

By imposing the boundary condition at $x = -\infty$, we find $D^i_2 = 0$, and the continuity condition determines D^i_3 to be

$$D^i_3 = D^i_1\ \operatorname{erfc}\left(\sqrt{\frac{k}{2}}d\right) + \frac{\sqrt{\frac{k}{2\pi}}l_i}{\operatorname{erfc}(\sqrt{\frac{k}{2}}d)}\, d\, e^{\frac{-kd^2}{2}}$$

Finally, D^i_1 can be obtained using (3.2) and it is given by

$$D^i_1 = \frac{-l_i}{2\ \operatorname{erfc}(\sqrt{\frac{k}{2}}d)}(1 + kd^2).$$

Thus, the steady state solutions for the enthalpy variables are

$$h_D = \begin{cases} \frac{-l_d}{2\ \mathrm{erfc}\left(d\sqrt{\frac{k}{2}}\right)}(1+kd^2)\ \mathrm{erfc}\left(-x\sqrt{\frac{k}{2}}\right) - \frac{l_d\sqrt{\frac{k}{2\pi}}}{\mathrm{erfc}\left(d\sqrt{\frac{k}{2}}\right)}\ x\ e^{\frac{kx^2}{2}} & x < -d \\ -\frac{l_d}{2}(1+kd^2) + \frac{l_d\sqrt{\frac{k}{2\pi}}}{\mathrm{erfc}\left(d\sqrt{\frac{k}{2}}\right)}\ d\ e^{\frac{kd^2}{2}} & -d < x < 0. \end{cases} \tag{3.27}$$

$$h_E = \begin{cases} \frac{-l_e}{2\ \mathrm{erfc}\left(d\sqrt{\frac{k}{2}}\right)}(1+kd^2)\ \mathrm{erfc}\left(-x\sqrt{\frac{k}{2}}\right) - \frac{l_e\sqrt{\frac{k}{2\pi}}}{\mathrm{erfc}\left(d\sqrt{\frac{k}{2}}\right)}\ x\ e^{\frac{kx^2}{2}} & x < -d \\ -\frac{l_e}{2}(1+kd^2) + \frac{l_e\sqrt{\frac{k}{2\pi}}}{\mathrm{erfc}\left(d\sqrt{\frac{k}{2}}\right)}\ d\ e^{\frac{kd^2}{2}} & -d < x < 0. \end{cases} \tag{3.28}$$

The final jump condition, (3.22a) or (3.22b), now determines an expression for the location of the flame, d, versus the strain rate of the flow, k. These jumps result in the following expressions to determine the flame response.

For $\phi_1 + h_E - h_D > 0$,

$$\sqrt{k} = \sqrt{\frac{\pi}{2}}\ \mathrm{erfc}(\beta)\ e^{\beta^2}\left(1+\mu\left(\frac{1}{2}+\beta^2-\frac{\beta e^{-\beta^2}}{\sqrt{\pi}\ \mathrm{erfc}(\beta)}\right)\right)^{\frac{1}{2}} e^{\frac{-l_d}{2}\left(\frac{1}{2}+\beta^2-\frac{\beta e^{-\beta^2}}{\sqrt{\pi}\ \mathrm{erfc}(\beta)}\right)} \tag{3.29}$$

and if $\phi_1 + h_E - h_D < 0$

$$\sqrt{k} = \sqrt{\frac{\pi}{2}}\ \mathrm{erfc}(\beta)\ e^{\beta^2}\left(\varphi-\mu\left(\frac{1}{2}+\beta^2-\frac{\beta e^{-\beta^2}}{\sqrt{\pi}\ \mathrm{erfc}(\beta)}\right)\right)^{\frac{1}{2}} e^{\frac{-l_e}{2}\left(\frac{1}{2}+\beta^2-\frac{\beta e^{-\beta^2}}{\sqrt{\pi}\ \mathrm{erfc}(\beta)}\right)+\frac{\phi_1}{2}}, \tag{3.30}$$

where $\phi_1 + h_E - h_D = \phi_1 + (l_d - l_e)(\frac{1}{2} + \beta^2 - \frac{\beta e^{-\beta^2}}{\sqrt{\pi}\ \mathrm{erfc}(\beta)})$. For convenience we have defined

$$\beta = \sqrt{\frac{k}{2}}\ d, \tag{3.31}$$

and also the parameters

$$\mu = \frac{l_d - l_e}{2A} \qquad\qquad \varphi = \frac{2 - \phi_1}{2 + \phi_1}.$$

As β ranges from zero to infinity, the standoff distance also varies monotonically over the same range. Thus, the response curve can be constructed in the following manner. By incrementing β from zero to infinity, (3.29) or (3.30), depending on the inequality, determines the strain rate, k. The standoff distance, d, is then found from (3.31). The curves in the d versus k plane are found to either decrease monotonically to $d = 0$, suggesting that the flame can be pushed all the way to the wall, or the curve possesses a turning point and becomes double valued. In this latter case, the turning point corresponds to an extinction point.

We have found that the flame response in stagnation point flow is determined by either (3.29) or (3.30) depending on the values of ϕ_1, l_i and k. For the uniformly strained flame considered here, i.e. k constant, the same equation determines the response along the entire flame surface. In other words, for a given set of parameters, the same species leaks through along the entire flame surface. In more general systems, however, it may be possible that some portions of the surface burn lean while neighboring areas burn rich. In such case, both equations play a role in the overall flame response.

To discuss the response curves for the uniformly strained flame, we will refer to (3.29) and (3.30) as Case 1 and Case 2, respectively. Case 1 corresponds to the situation when the initially deficient reactant is consumed by the flame, and Case 2 is appropriate when the initially excess reactant is consumed. Predicted response curves for different parameter values will now be discussed in turn.

3.2.1 Off-stoichiometric mixtures

When conditions are far removed from stoichiometry, $\phi_1 \to \infty$, it is clear that $\phi_1 + h_E - h_D > 0$ and thus Case 1 always determines the flame response. In this limit, $\mu \to 0$ and the single reactant theory of Buckmaster [16] is recovered which depends only on l_d. Typical response curves are shown in figure 3.3 for several different values of l_d. We observe the following: for weak strain rate, the flame resides far from the stagnation plane, i.e. $d \gg 1$ and the flame structure resembles that of a planar flame in a uniform flow. As the strain rate is increased, the flame is pushed closer to the wall. When the deviation from unity of the deficient Lewis number, l_d, is less than four, the response is monotonic, suggesting that the flame can be pushed all the way down to the wall before it is extinguished. When l_d is greater than four, the response curve becomes double-valued. The turning point observed in the corresponding curves is regarded as the extinction point. When the strain rate exceeds the critical value at the turning point, the system can no longer support a planar flame and extinction occurs. The lower portion of the curve, below the extinction point, is presumed to be unstable.

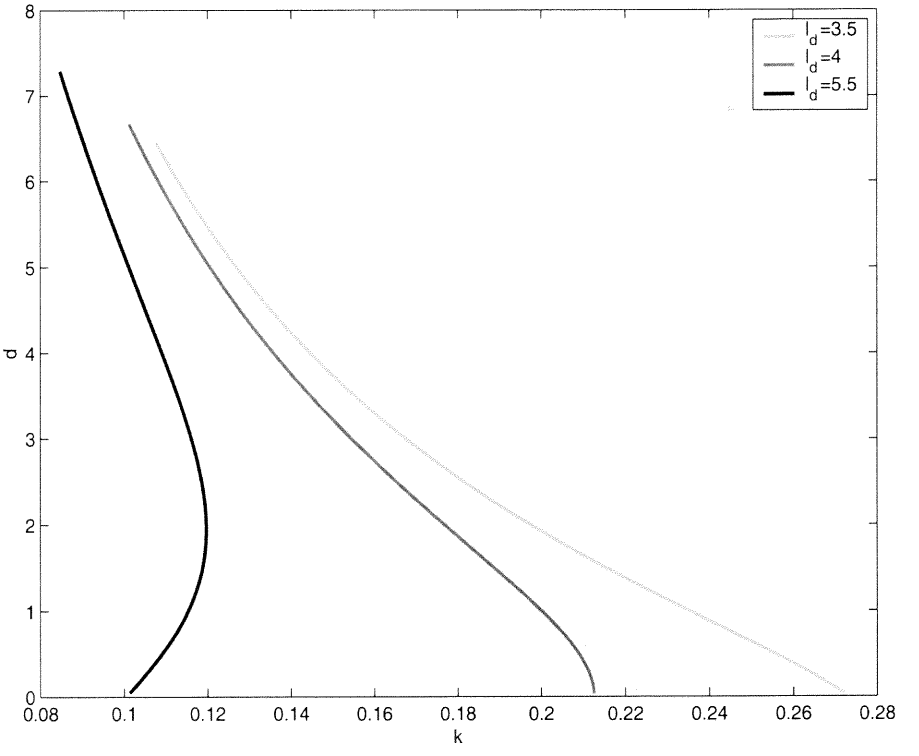

Figure 3.3: Standoff distance versus strain rate for off-stoichiometric mixtures

The flame speed, S_f° defined to be the speed of the flame relative to the underlying flow field, is simply the normal velocity of the incoming flow evaluated at the reaction sheet, i.e. $S_f^\circ = kd$. Curves illustrating the dependence of S_f° on k are shown in figure 3.4 for several values of l_d. Again we observe that $l_d = 4$ is the critical condition determining the response. For $l_d > 4$ the curves are double-valued and the turning point refers to an extinction point. However, for $l_d < 4$ the flame speed will eventually be reduced to zero for sufficiently large k. We also observe that the flame speed of the strained flame will exceed the adiabatic flame speed, $S_f^\circ = 1$, when l_d is sufficiently small. This is consistent with previous studies of flame response to straining, c.f. [6].

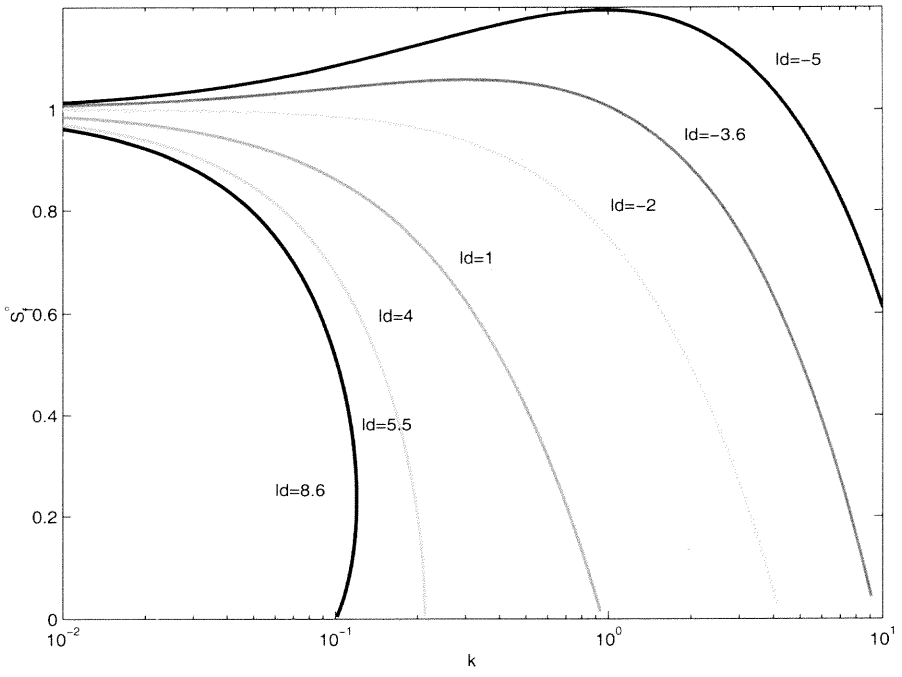

Figure 3.4: Flame speed versus strain rate

3.2.2 Weakly-strained flames

When the flame is weakly strained, $k \ll 1$, the flame retreats far from the stagnation plane, and $d \to \infty$. Equations (3.29) and (3.30) determine that $\beta \to \infty$, and thus again the inequality $\phi_1 + h_E - h_D > 0$ for any non-zero ϕ_1. Therefore Case 1 is always the appropriate condition to determine flame behavior. For weak strain rate, Case 1 determines the flame position as

$$d = \frac{1}{k} + \left(\frac{\mu - l_d}{2} - 1 \right) + O(1),$$

and therefore the flame speed takes the form

$$S_f^\circ = 1 - \left(1 + \frac{l_d - \mu}{2} \right) k + O(k).$$

We see that the flame speed will exceed its adiabatic value when $l_d - \mu < -2$. When conditions are far removed from stoichiometry, $\mu \to 0$, and this inequality reduces to $l_d < -2$, consistent with the curves shown in figure 3.4. We conclude that

weakly-strained flames will always be governed by Case 1. These flames reside far from the stagnation plane and their structure is essentially that of a planar flame in a uniform flow field. Consequently, the initially deficient reactant remains deficient everywhere in the flow field and is ultimately consumed at the flame. However, when $O(1)$ straining is considered, and conditions are close to stoichiometry, it is possible for the initially deficient reactant to be locally abundant at the reaction sheet. As a result, a small amount of this reactant leaks through, and Case 2 becomes the relevant equation to determine flame response. This scenario is discussed next.

3.2.3 Near-stoichiometric strained flames

First, consider the following function appearing in the inequality

$$\phi_1 + (l_d - l_e)\Gamma,$$

where

$$\Gamma = \frac{1}{2} + \beta^2 - \frac{\beta e^{-\beta^2}}{\sqrt{\pi}\ \mathrm{erfc}(\beta)}.$$

The sign of this function determines whether Case 1 or Case 2 is to be used. Recall that the response curves of d vs. k range from $d = 0$ to $d = \infty$, and they are generated by incrementing β from 0 to ∞. That is, d close to 0 corresponds to $\beta \to 0$ and large d corresponds to $\beta \to \infty$. The limiting values of Γ are readily found to be: $\Gamma \to 1/2$ as $\beta \to 0$ and $\Gamma \to 0$ as $\beta \to \infty$. It is possible, then, that for fixed values of l_i and ϕ_1, the top portion of the curves d vs. k are determined by Case 1 and the lower portion by Case 2. Different scenarios are discussed next.

$\underline{\mathbf{l_d > l_e}}$

As defined, ϕ_1 is always positive, and we have determined that Γ is also positive. Therefore, when $l_d > l_e$, Case 1 is always valid. The Lewis number of the deficient reactant is larger, suggesting that this reactant is less mobile than the excess reactant.

It does not diffuse as readily across the strained flow field and always remains deficient. Although Case 1 remains valid, both Lewis numbers play a role in the flame behavior. This is illustrated in figure 3.5 where the flame position is shown as a function of strain rate for fixed $l_d = 5.5$ and $l_e = -8.0$ with $\phi_1 = 0.2$. The single reactant theory predicts that this flame response should be double valued, and the flame should extinguish at a finite distance from the wall (see figure 3.3). However, that conclusion is only valid far from stoichiometry, and in fact we observe that for conditions closer to stoichiometry, the response is monotonic and no extinction point is predicted.

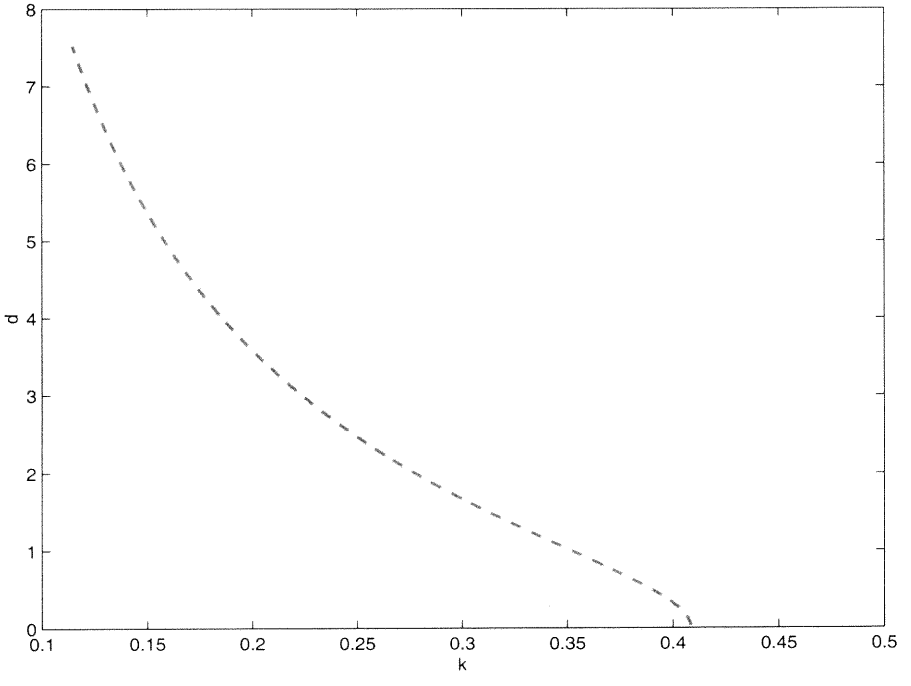

Figure 3.5: Standoff distance versus strain rate for $l_d = 5.5$, $l_e = -8$ and $\phi_1 = 0.2$.

$\underline{\mathbf{l_d < l_e}}$

The most interesting situation occurs when $l_d < l_e$. In this case, the initially abundant reactant is the less mobile of the two, and will not diffuse as rapidly toward the reaction sheet. As a result, this reactant can become locally deficient in the vicinity of the reaction zone. It is therefore consumed, and Case 2 determines the flame response. Figures 3.6-3.9 show how the flame response is modified by different

diffusivities. Figures 3.6 and 3.7 are drawn with fixed $l_d = 4.0$ and two different values of ϕ_1 for several values of l_e. The dashed portion of each curve represents the segment determined by Case 1, while the solid portions show where Case 2 is appropriate. We see from Figures 3.6 and 3.7, for example, that for a given ϕ_1 and fixed l_d Case 1 remains valid along the entire curve provided l_e is less than some critical value. However, once l_e exceeds this value, Case 1 is only used to determine the top part of each curve, while Case 2 becomes the governing condition on the bottom part.

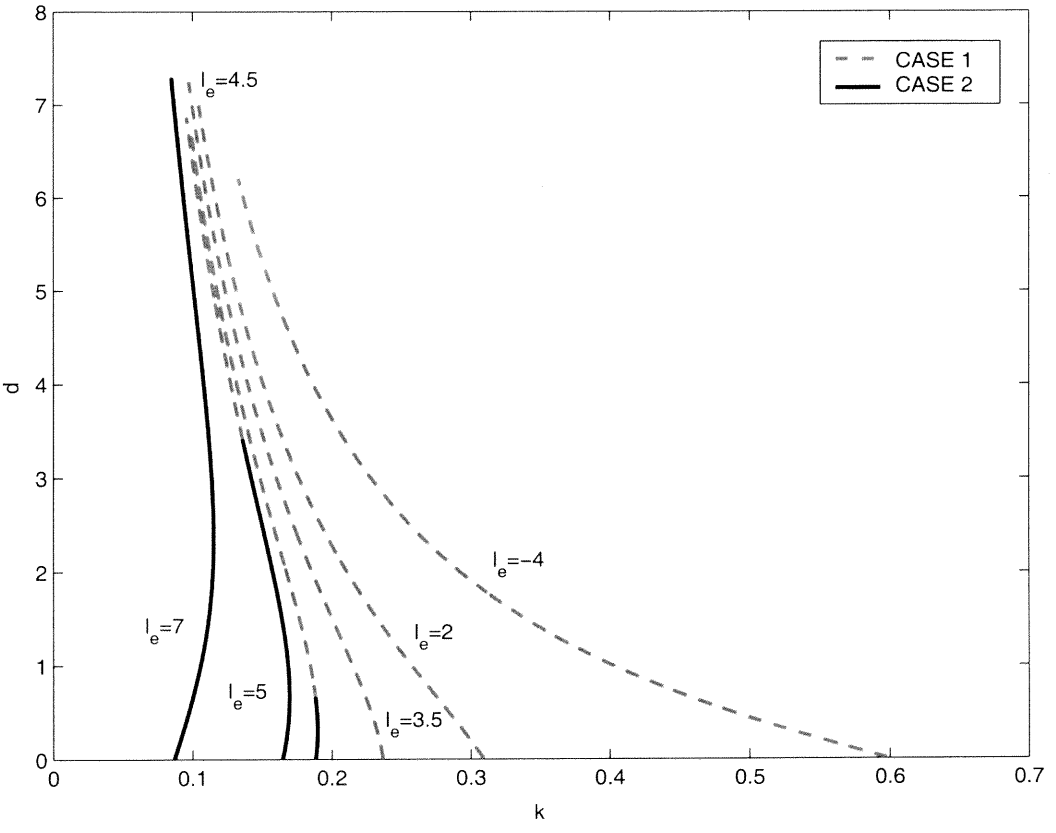

Figure 3.6: Standoff distance versus strain rate for several l_e with $l_d = 4$ and $\phi_1 = 0.2$. The dashed curves indicate the response is determined by (3.29) and solid curves indicate the response is determined by (3.30)

.

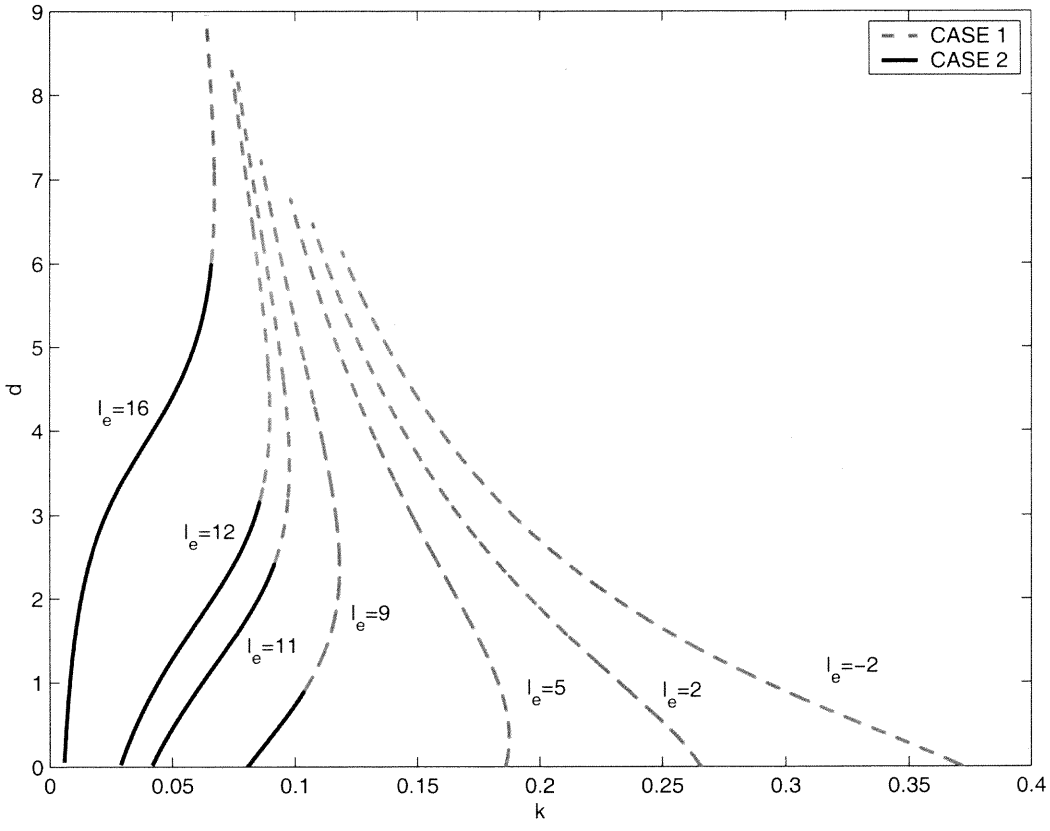

Figure 3.7: Standoff distance versus strain rate for several l_e with $l_d = 4$ and $\phi_1 = 2$.

Figures 3.8 and 3.9 show similar plots, but with fixed l_e for various l_d. We observe that Case 2 becomes relevant along the bottom of the curves when l_d drops below a critical value. As discussed earlier, Γ decreases monotonically as d increases from 0 to ∞. Therefore, when Case 2 becomes relevant, it will always be valid on the lower portion of the curve, i.e. when the flame approaches the wall. The low mobility of the initially excess reactant prevents it from diffusing quickly enough across the strained flow field and it becomes locally deficient, and hence consumed, at the reaction sheet. As the flame moves further away from the wall, Case 1 will eventually take over as the strain rate is weakened. We note that in situations where the curve becomes double-valued, the transition from Case 1 to Case 2 may either occur before or after the turning point. When the transition occurs below the turning point, extinction will have already occurred, and the transition will in fact not be

observed. However, when the transition occurs above the turning point, extinction will be determined by Case 2.

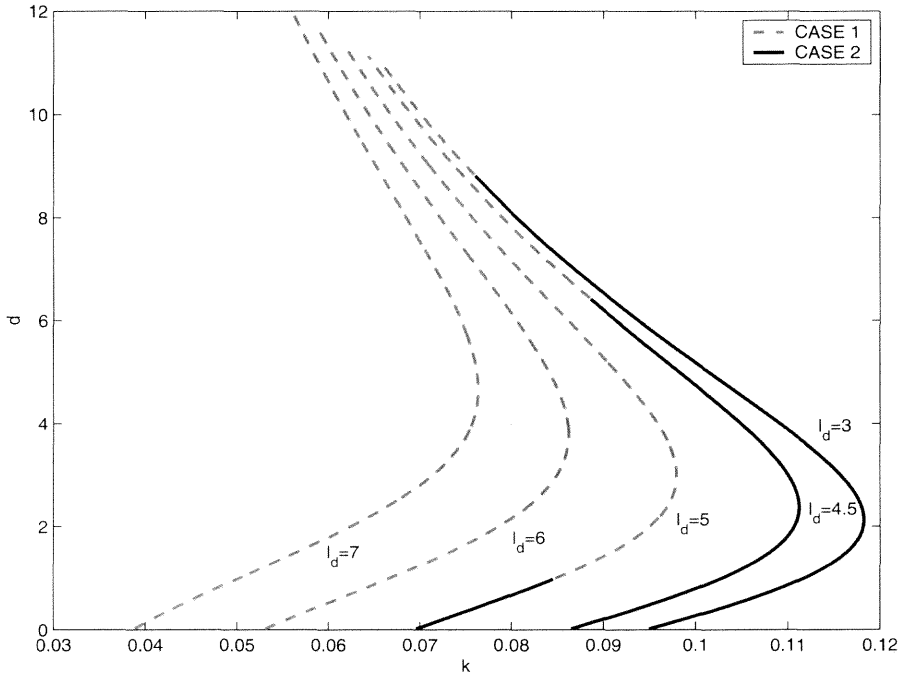

Figure 3.8: Standoff distance versus strain rate for $l_e = 6.5$ and $\phi_1 = 0.2$

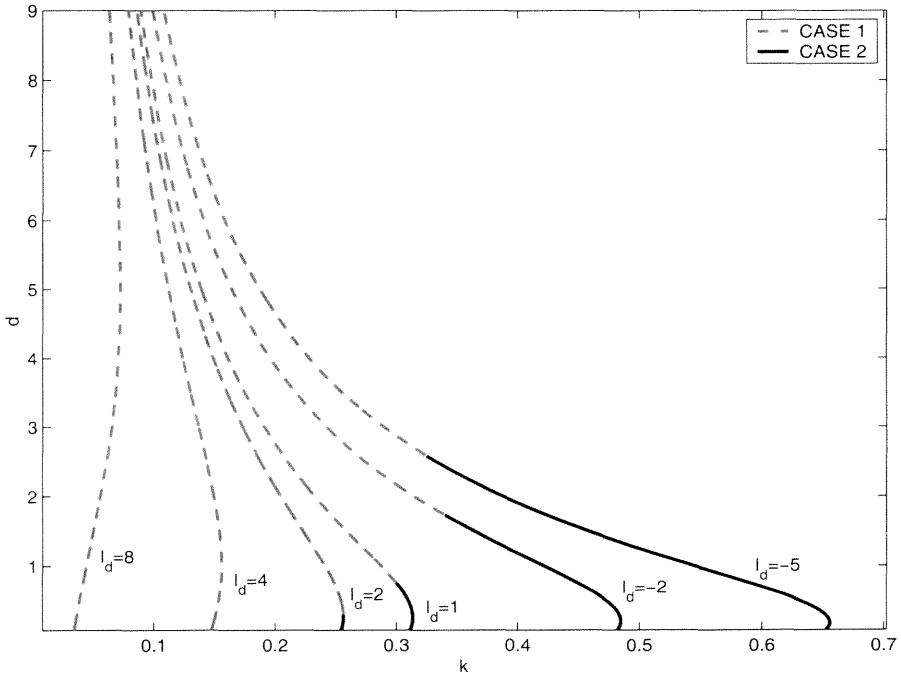

Figure 3.9: Standoff distance versus strain rate for $l_e = 6.5$ and $\phi_1 = 2$

All the curves seem to indicate that the transition from Case 1 to Case 2 is quite smooth. However, one must account for this transition to correctly predict the qualitative flame response. To illustrate this point, we show in figure 3.10 two curves of flame position versus strain rate for $l_d = -2.0, l_e = 6.0$ and $\phi_1 = 3.0$. In this case, the transition occurs at approximately $k = 0.78$, (denoted by $*$ on the curve), below which point Case 2 takes over. The solid curve shows that the flame will be pushed all the way to the wall. However, if Case 1 were used instead, a turning point, and hence extinction, would be incorrectly predicted.

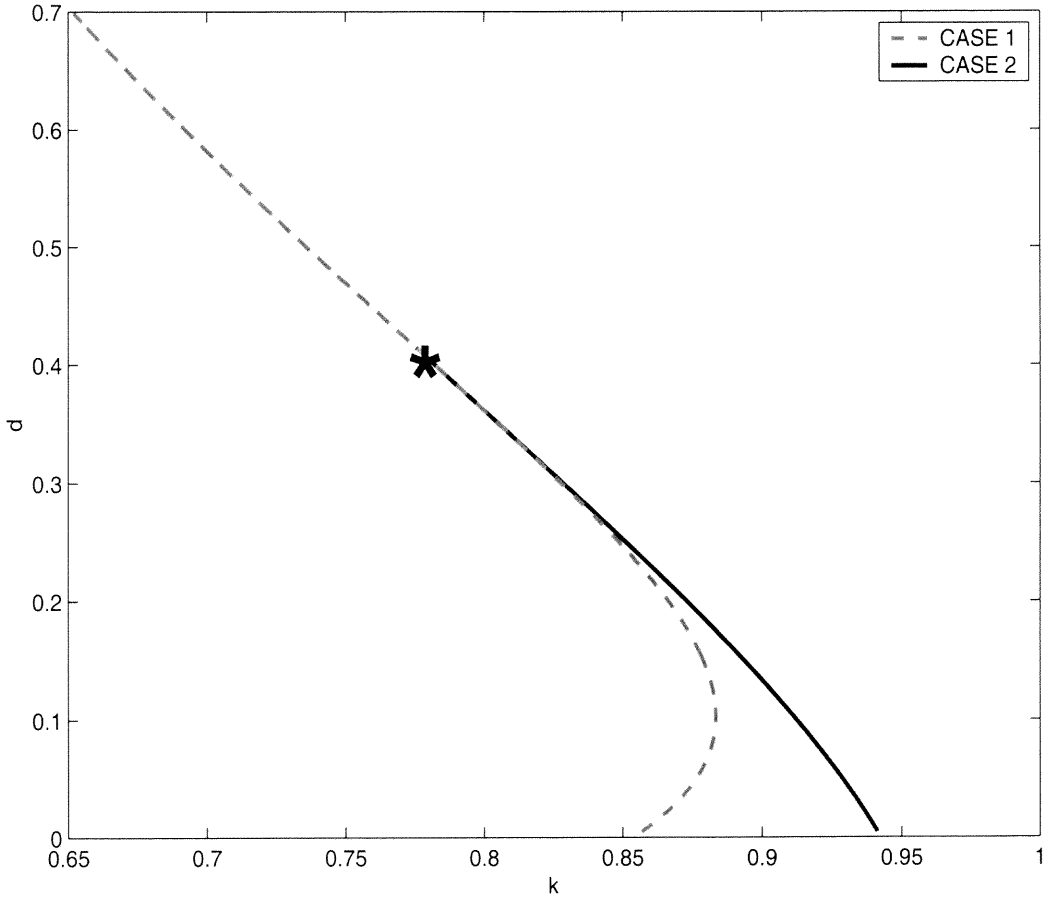

Figure 3.10: Standoff distance versus strain rate for $l_d = -2$, $l_e = 6$ and $\phi_1 = 3$. The $*$ indicates transition from (3.29) to (3.30), i.e. where abundant reactant becomes deficient

3.2.4 Effect of Equivalence Ratio

Recall that the effects of stoichiometry are measured in terms of ϕ_1, which is the deviation from unity of the ratio of excess-to-deficient reactants. Also, as defined, ϕ_1 is always positive. Note that the deviation from unity of the equivalence ratio, Φ_1, is related to ϕ_1 in the following way

$$\phi_1 = \begin{cases} \Phi_1 & \text{rich mixtures} \\ -\Phi_1 & \text{lean mixtures.} \end{cases}$$

For a given fuel mixture, the roles of l_d and l_e are reversed as stoichiometry is crossed. That is, for lean mixtures l_d and l_e assume the values of l_F and l_O, respectively. However, when the mixture composition is altered to become fuel rich, $l_d = l_O$ and $l_e = l_F$. It follows from our discussion above, that Case 1 will always be valid on one side of stoichiometry while Case 2 will be valid on the other, at least in the immediate vicinity of $\Phi_1 \approx 0$. Of course, as conditions move sufficiently far away from stoichiometry, Case 1 always takes over. As discussed, Γ assumes its largest value of $1/2$ at $d = 0$. In order for Case 2 to play a role in the response curve the following inequality must be satisfied:

$$\phi_1 + (l_d - l_e)/2 < 0.$$

As an example, consider a mixture with

$$l_F = 6.0, \quad l_O = 2.0.$$

For lean mixtures, $l_d = 6.0$, $l_e = 2.0$, and it follows that $\phi_1 + (l_d - l_e)/2 > 0$. Therefore the entire flame response is determined by Case 1. For rich mixtures, $l_d = 2.0$, $l_e = 6.0$, and the above inequality indicates that Case 2 will be used to generate the lower part of the response curves for $0 < \Phi_1 < 2.0$. Beyond $\Phi_1 = 2.0$ Case 1 is again always the relevant case. This is illustrated in figure 3.11 where we

show the extinction standoff distance as a function of the deviation from unity of equivalence ratio. On the lean side, extinction is determined by Case 1, while on the rich side Case 2 is relevant.

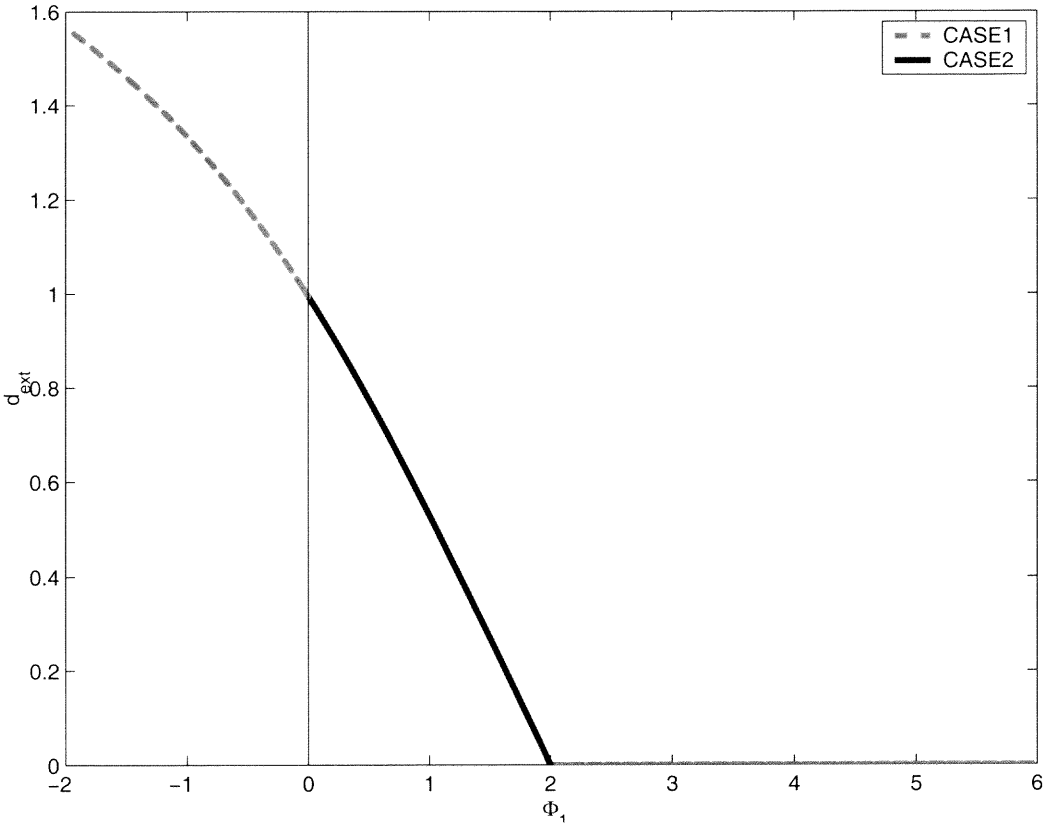

Figure 3.11: Standoff distance at extinction versus deviation from unity of the equivalence ratio for $l_F = 6$, $l_O = 2$

Extinction

It has been shown that extinction can be described by either Case 1 or Case 2. For off-stoichiometric mixtures, we found that $l_d = 4$ is the critical value that separates the double-valued response ($l_d > 4$) from the single-valued response ($l_d < 4$). Here we seek critical conditions for extinction appropriate for conditions closer to stoichiometry.

When Case 1 is valid, it follows from (3.29) that the strain rate at which the flame is at the wall is given by

$$k = \frac{\pi}{2}(1 + \mu/2)e^{-l_d/2}.$$

When a turning point first develops the slope at this point of intersection will be infinite, and upon differentiating (3.29) we find that this occurs at

$$l_d + \frac{2\mu}{2+\mu} = 4.$$

The following response is therefore predicted:

$$l_d + \frac{2\mu}{2+\mu} < 4, \quad \text{single-valued,}$$

$$l_d + \frac{2\mu}{2+\mu} > 4, \quad \text{double-valued.}$$

When Case 2 is valid, the value of the strain rate when $d = 0$ is found from (3.30) to be

$$k = \frac{\pi}{2}(\varphi - \mu/2)e^{-l_e/2+\phi_1}.$$

We also find the following predicted responses:

$$l_e + \frac{2\mu}{2\varphi - \mu} < 4, \quad \text{single-valued,}$$

$$l_e + \frac{2\mu}{2\varphi - \mu} > 4, \quad \text{double-valued.}$$

Now consider typical response curves as a function of equivalence ratio for the parameter values $l_F = 6.0$, $l_O = 0.0$. For lean mixtures, $l_d = 6.0$, $l_e = 0.0$, we have $\phi_1 + (l_d - l_e)/2 > 0$ and therefore the entire response is determined by Case

1. Furthermore, we determined that $l_d + \frac{2\mu}{2+\mu} > 4$, so that the response is always double-valued. For rich mixtures, $l_d = 0.0$, $l_e = 6.0$, and we find that Case 2 will determine part of the response curve when $0 < \Phi_1 < 3.0$, and Case 1 is valid otherwise. The above inequalities also determine that the response is double-valued when $0 < \Phi_1 < 2.0$. Beyond $\Phi_1 = 2.0$ the response is single-valued.

In figure 3.12, we show the extinction and transition stand-off distances as a function of equivalence ratio for $l_F = 6.0$ and $l_O = 0.0$. Recall that $\Phi_1 = (\hat{\Phi} - 1)/\epsilon Q$ is equal to $-\phi_1$ for lean and $+\phi_1$ for rich mixtures. In the figure d_T denotes the flame position at which the transition occurs. The shaded region indicates that Case 2 is used, while in the remaining regions Case 1 valid. The curve d_{ext} shows the stand-off distance at extinction, i.e. at the turning point. The dashed part of the curve indicates that Case 1 determines the extinction condition, while the solid part indicates that Case 2 is valid. Thus, the response is monotonic for all $\Phi_1 > 2$ and double-valued for $\Phi_1 < 2$. Extinction is governed by Case 2 for $0 < \Phi_1 < 2$ and by Case 1 for $\Phi_1 < 0$.

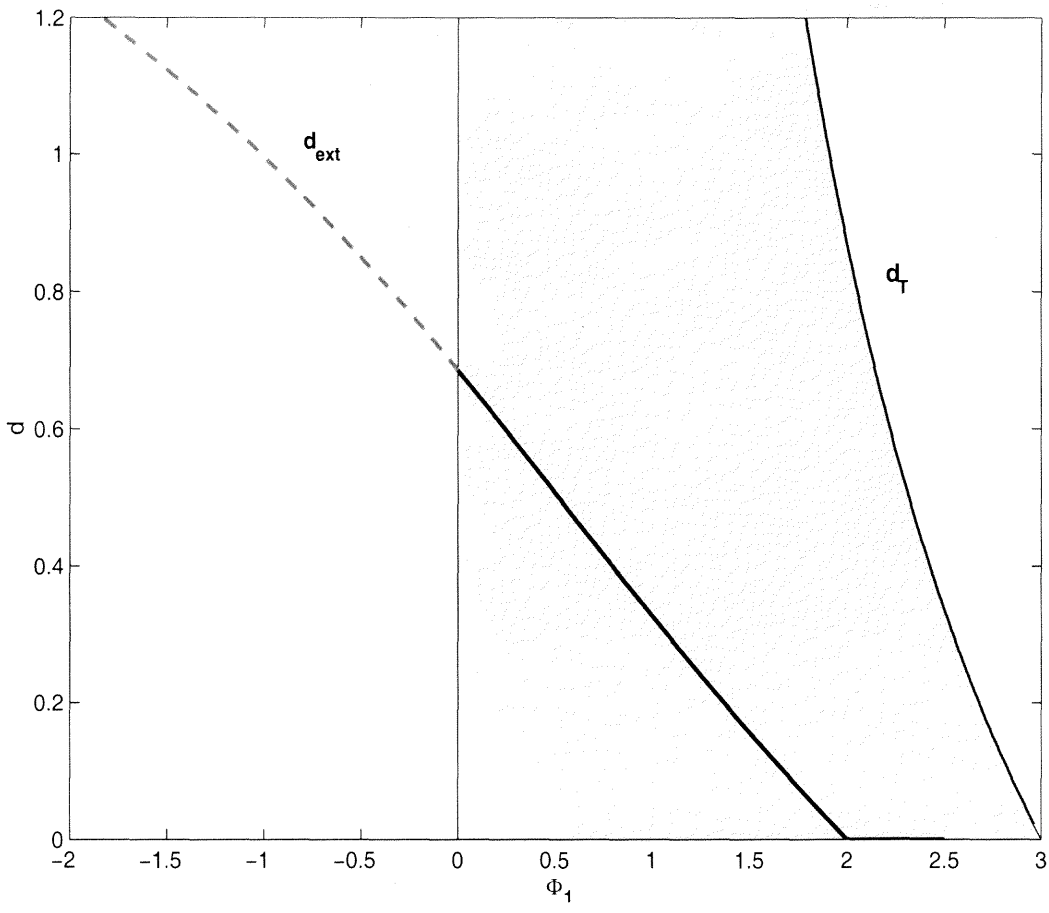

Figure 3.12: Extinction and transition standoff distances versus deviation from the equivalence ratio for $l_F = 6$ and $l_O = 0$. In the shaded region, d is determined by (3.30).

Similar curves are shown in figures 3.13-3.15 for various parameter values. In general when the Lewis number of the fuel sufficiently exceeds that of the oxidant, the response is monotonic when the mixture is sufficiently rich, and double-valued otherwise. The response is typical of heavy hydrocarbons such as propane and butane. On the other hand, when the fuel Lewis number is less than that of the oxidant, the response is monotonic only if the mixture is sufficiently lean. These curves showing d_{ext} as a function of equivalence ratio are consistent with the experimental results of Yamaoka and Tsuji [17] on methane-air flames, as well as the theory presented in [15].

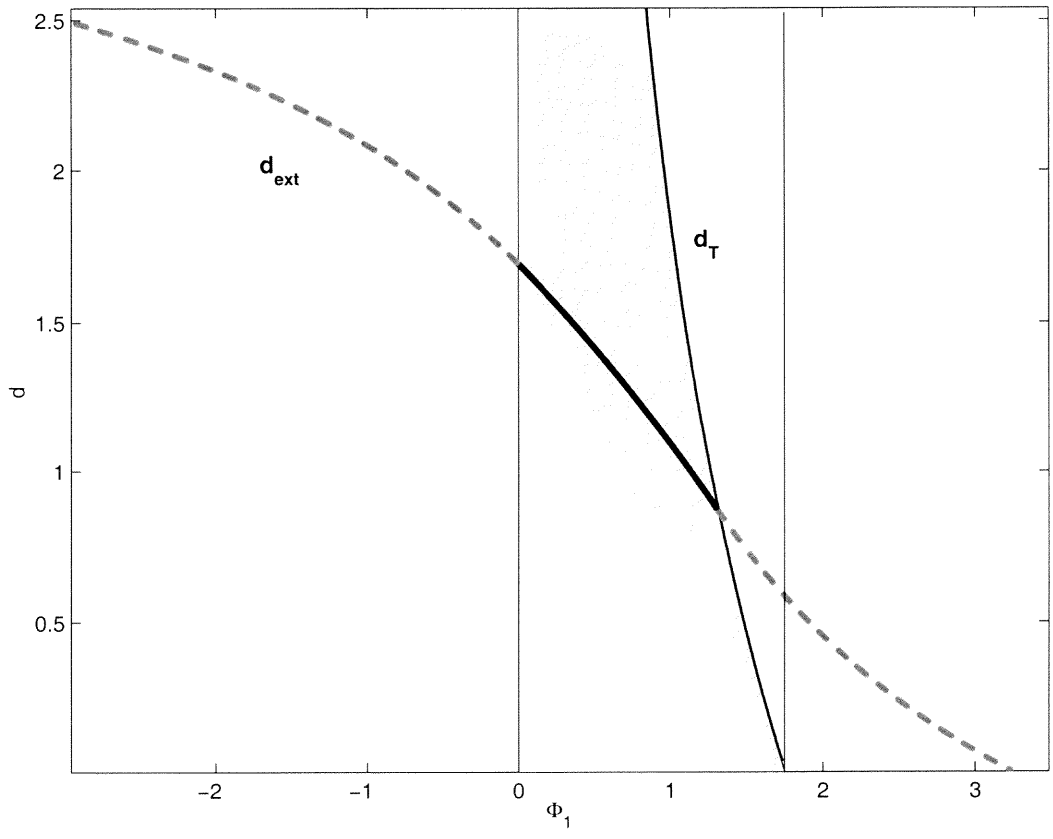

Figure 3.13: Extinction and transition standoff distances versus deviation from the equivalence ratio for off stoichiometric mixtures where $l_F = 6.5$ and $l_O = 3$

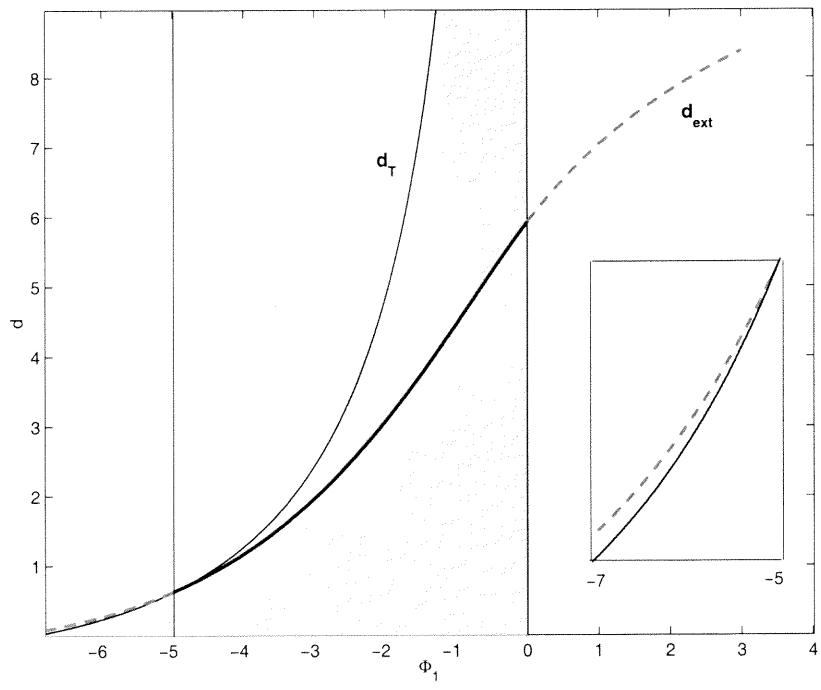

Figure 3.14: Extinction and transition standoff distances versus deviation from the equivalence ratio for off stoichiometric mixtures where $l_F = -2$ and $l_O = 12$. The insert shows a blow up of the plot to the left of $\Phi_1 = -5$.

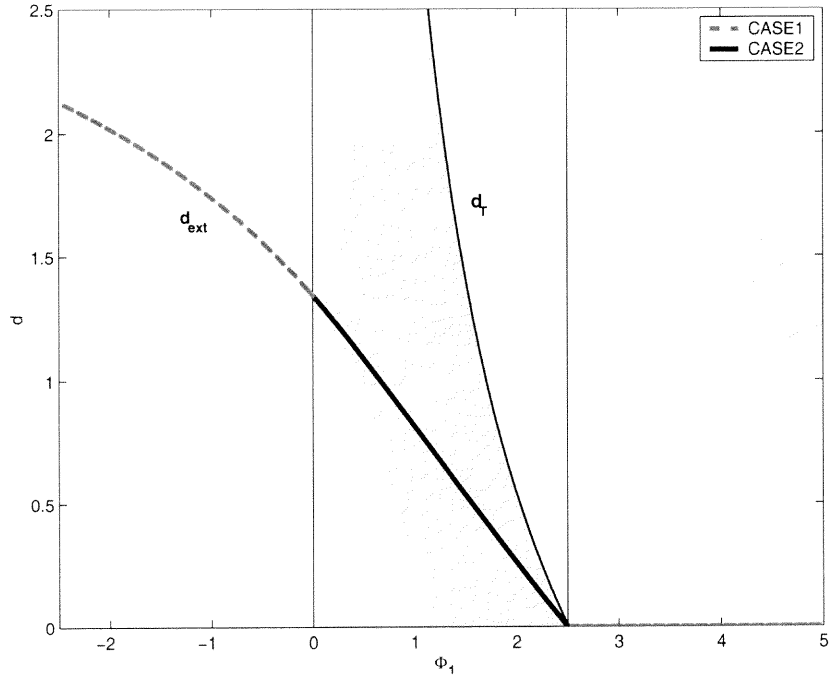

Figure 3.15: Extinction and transition standoff distances versus deviation from the equivalence ratio for off stoichiometric mixtures where $l_F = 6.5$ and $l_O = 1.5$

Flame speed

The flame speed is defined exactly as was done for the off-stoichiometric flames, i.e. $S_f^\circ = kd$. Typical plots of S_f° vs. k are shown in figure 3.16 for several values of l_d with $le = 6.5$ and $\phi_1 = 2$. As before, the dashed segments correspond to Case 1 and the solid segments to Case 2. By comparing the curve in figure 3.4 and 3.16 for $l_d = -5$, we see that the predicted response can be quite different when conditions are closer to stoichiometry.

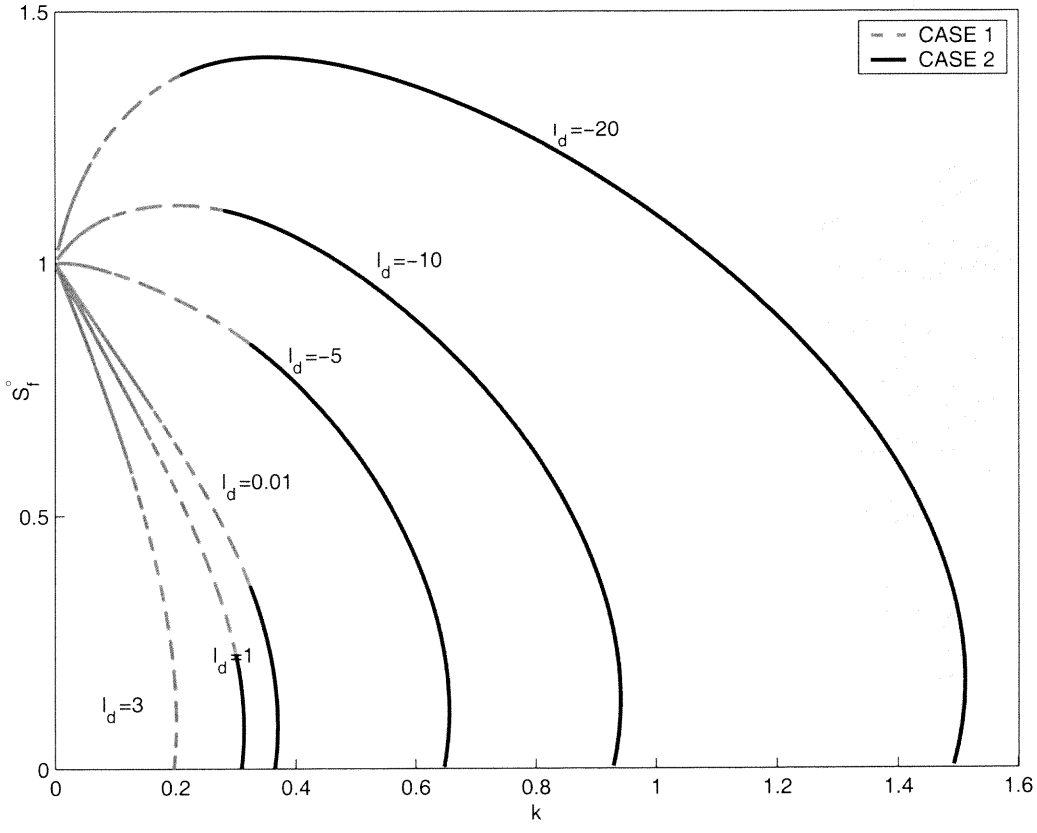

Figure 3.16: Flame speed versus strain rate

3.2.5 Weakly Non-Linear Analysis of Strained Flames

Here the derivation of a non-linear partial differential equation is outlined which describes the evolution of the strained flame near the cellular stability boundary (figure 3.1) for our model given by (2.57)-(2.64). A similar analysis was done in [18]

within the framework of a single reactant theory, and other analyses have been done for many problems that exhibit long wave instabilities. Here we explore modifications that may arise due to the competing species. Once we first cross the stability threshold, linear theory predicts that the flame will lose stability to a cellular structure. The theory, however, does not determine the ultimate fate of these perturbations. Our objective here is to perform a non-linear stability analysis about this point for $k \ll 1$.

We start by determining the appropriate scaling of our variables. Recall the transcendental equation obtained earlier, (3.29), that related the strain rate and the standoff distance for weak stretch where the locally deficient reactant was consumed behind the flame:

$$\sqrt{k} = \sqrt{\frac{\pi}{2}}\,\mathrm{erfc}(\beta)e^{\beta^2}\left(1+\mu(\frac{1}{2}+\beta^2-\frac{\beta e^{-\beta^2}}{\sqrt{\pi}\,\mathrm{erfc}(\beta)})\right)^{\frac{1}{2}} e^{\frac{-l_D}{2}\left(\frac{1}{2}+\beta^2-\frac{\beta e^{-\beta^2}}{\sqrt{\pi}\,\mathrm{erfc}(\beta)}\right)}.$$

From this equation it follows that for $k \ll 1$, β must be large which in turn implies that d is large. Upon substituting the expansion

$$\mathrm{erfc}(\beta) \sim \frac{1}{\sqrt{\pi}}\,e^{-\beta^2}\left(\frac{1}{\beta}-\frac{1}{2\beta^3}+\frac{3}{4\beta^5}+\cdots\right) \tag{3.32}$$

into (3.29) we get the following:

$$\begin{aligned}\sqrt{2k} \;\sim\; & \left(\frac{1}{\beta}-\frac{1}{2\beta^3}+\frac{3}{4\beta^5}\right)\left[1+\mu\left(\frac{1}{2}+\beta^2-\frac{\beta}{\frac{1}{\beta}-\frac{1}{2\beta^3}+\frac{3}{4\beta^5}}\right)\right]^{\frac{1}{2}} \\ & e^{\frac{-l_d}{2}\left(\frac{1}{2}+\beta^2-\frac{\beta}{\frac{1}{\beta}-\frac{1}{2\beta^3}+\frac{3}{4\beta^5}}\right)}.\end{aligned} \tag{3.33}$$

By further expanding this expression for large β we have

$$\sqrt{2k} \sim \frac{1}{\beta}\left[1+\frac{1}{\beta^2}\left(\frac{-1}{2}+\frac{\mu}{4}-\frac{l_d}{4}\right)\right]. \tag{3.34}$$

Equation (3.34), together with the definition of β (3.31) suggests the scaling on the standoff distance, d, to be

$$d = \frac{1}{k} + \left(\frac{\mu - l_D}{2} - 1\right) + o(1). \tag{3.35}$$

When the stain rate is zero, i.e. $k = 0$, the standoff distance $d \to \infty$ and we essentially recover the planar flame in uniform flow. In that case, analysis shows that instability sets in when the following is true:

$$l_c = l_d - \mu < -2 \tag{3.36}$$

where $\mu = \frac{l_d - l_e}{2+\phi_1}$. A splitting parameter ϵ is defined as

$$\epsilon = \frac{-l_c}{2} - 1,$$

and the dispersion relation now suggests the following spatial and temporal scales

$$\tau = \epsilon^2 t \qquad \eta = \sqrt{\epsilon} y \qquad \zeta = \sqrt{\epsilon} z.$$

Finally, the strain rate, k and the mixture strength parameter, ϕ_1, are scaled as

$$k = \epsilon^2 \alpha, \quad \phi_1 = \epsilon^2 \varphi.$$

The above expansions are inserted into our system and we will look for solutions in the following form:

$$\tau = \tau^s + \epsilon^2(\theta_0 + \epsilon\theta_1) + \cdots \qquad f = 0 + \epsilon(F_0 + \epsilon F_1) + \cdots$$

$$h^D = h_s^D + \epsilon^2(S_0 + \epsilon S_1) + \cdots \qquad h^E = h_s^E + \epsilon^2(R_0 + \epsilon R_1) + \cdots.$$

Once we insert the assumed forms of solutions into our system, we obtain the following equations at $O(\epsilon^2)$:

$$\frac{\partial \theta_0}{\partial \xi} - \frac{\partial^2 \theta_0}{\partial^2 \xi^2} = -\frac{d\tau^s}{d\xi}(F^0_{\eta\eta} + F^0_{\zeta\zeta}), \quad \xi < 0$$

$$\theta_0 = 0, \quad 0 < \xi < d$$

$$\frac{\partial S_0}{\partial \xi} - \frac{\partial^2 S_0}{\partial^2 \xi^2} = l_d \left(\frac{\partial^2 \theta_0}{\partial^2 \xi^2} - \frac{d\tau^s}{d\xi}(F^0_{\eta\eta} + F^0_{\zeta\zeta}) \right) + \frac{dh^s_D}{d\xi} \left(\alpha\xi - F^0_{\eta\eta} - F^0_{\zeta\zeta} \right), \quad \xi < 0$$

$$\frac{\partial S_0}{\partial \xi} - \frac{\partial^2 S_0}{\partial^2 \xi^2} = \frac{dh^s_D}{d\xi} \left(\alpha\xi - F^0_{\eta\eta} - F^0_{\zeta\zeta} \right), \quad 0 < \xi < d$$

$$\frac{\partial R_0}{\partial \xi} - \frac{\partial^2 R_0}{\partial^2 \xi^2} = l_e \left(\frac{\partial^2 \theta_0}{\partial^2 \xi^2} - \frac{d\tau^s}{d\xi}(F^0_{\eta\eta} + F^0_{\zeta\zeta}) \right) + \frac{dh^s_E}{d\xi} \left(\alpha\xi - F^0_{\eta\eta} - F^0_{\zeta\zeta} \right), \quad \xi < 0$$

$$\frac{\partial S_0}{\partial \xi} - \frac{\partial^2 S_0}{\partial^2 \xi^2} = \frac{dh^s_E}{d\xi} \left(\alpha\xi - F^0_{\eta\eta} - F^0_{\zeta\zeta} \right), \quad 0 < \xi < d$$

$$[\theta_0] = 0 \qquad [S_0] = 0 \qquad [R_0] = 0$$

$$\left[\frac{d\theta_0}{d\xi} \right] = \frac{-(R_0 + S_O)}{4}$$

$$\left[\frac{dS_0}{d\xi} \right] = -l_d \left[\frac{d\theta_0}{\partial \xi} \right] \qquad \left[\frac{dR_0}{d\xi} \right] = -l_e \left[\frac{d\theta_0}{\partial \xi} \right]$$

$$\theta_0 = 0 \quad \text{as} \quad \xi \to -\infty, \qquad S_0 = 0 \quad \text{as} \quad \xi \to -\infty, \qquad R_0 = 0 \quad \text{as} \quad \xi \to -\infty.$$

The jump condition for the temperature gradient is obtained from (2.63a,b). Note that

$$\phi_1 + h_E - h_D = \epsilon^2(\varphi + R_0 - S_0),$$

and thus the sign of $\varphi + R_0 - S_0$ determines which species leaks through the flame surface. However, with the scalings used here, both jumps lead to the same expression for $\left[\frac{d\theta_0}{d\xi}\right]$. The steady state solutions of this system were derived earlier and are given by (3.1) - (3.3). A solution to the above system can now be constructed yielding the following:

$$\theta_0 = \begin{cases} (F^0_{\eta\eta} + F^0_{\zeta\zeta})\xi e^\xi + \alpha\xi e^\xi - \frac{1}{2}\alpha\xi^2 e^\xi & \xi < 0 \\ \\ 0 & 0 < \xi < d, \end{cases}$$

$$S_0 = \begin{cases} -l_d(F^0_{\eta\eta} + F^0_{\zeta\zeta})e^\xi - \alpha l_D e^\xi - \frac{1}{2} l_D \xi^2 e^\xi - l_d(F^0_{\eta\eta} + F^0_{\zeta\zeta})\xi^2 e^\xi \\ \quad + \frac{1}{2}\alpha l_d \xi^3 e^\xi & \xi < 0 \\ \\ -l_d(F^0_{\eta\eta} + F^0_{\zeta\zeta}) - \alpha l_d & 0 < \xi < d, \end{cases}$$

$$R_0 = \begin{cases} -l_e(F^0_{\eta\eta} + F^0_{\zeta\zeta})e^\xi - \alpha l_e e^\xi - \frac{1}{2} l_e \xi^2 e^\xi - l_e(F^0_{\eta\eta} + F^0_{\zeta\zeta})\xi^2 e^\xi \\ \quad + \frac{1}{2}\alpha l_e \xi^3 e^\xi & \xi < 0 \\ \\ -l_e(F^0_{\eta\eta} + F^0_{\zeta\zeta}) - \alpha l_e & 0 < \xi < d. \end{cases}$$

Note that the inequality that determines which species leaks through is given by

$$\varphi + (l_d - l_e)(F^0_{\eta\eta} + F^0_{\zeta\zeta} + \alpha) \gtrless 0. \tag{3.37}$$

Thus, the curvature of the front plays a large role in determining which species leaks through. However, since the jump conditions are identical for the two cases at this order, the flame dynamics will be the same regardless of whether a particular region burns rich or lean. This is above solution is expressed in terms of the perturbed front location F^0 which is not yet determined. We must, therefore, go to the next order of our perturbation scheme. This new system of $O(\epsilon^3)$ is just an inhomogeneous form of the leading order scheme and it's given by:

$$\begin{aligned}\frac{\partial \theta_1}{\partial \xi} - \frac{\partial^2 \theta_1}{\partial^2 \xi^2} &= e^{\xi}\left(F^0_{\tau} - F^1_{\eta\eta} - F^1_{\zeta\zeta} + (F^0_{\eta})^2 + (F^0_{\zeta})^2 - \alpha + \alpha F^0 + \alpha\eta F^0_{\eta}\right) \\ &\quad + \xi e^{\xi}(F^0_{\eta\eta\eta\eta} + F^0_{\zeta\zeta\zeta\zeta}) + 2\xi e^{\xi} F^0_{\eta\eta\zeta\zeta}, \qquad \xi < 0\end{aligned}$$

$$\theta_1 = 0, \qquad 0 < \xi < d$$

$$\begin{aligned}\frac{\partial S_1}{\partial \xi} - \frac{\partial^2 S_1}{\partial^2 \xi^2} &= l_d e^{\xi}\left(-F^0_{\tau} - (F^0_{\eta})^2 - (F^0_{\zeta})^2 - F^0_{\eta\eta\eta\eta} - F^0_{\zeta\zeta\zeta\zeta} - 2F^0_{\eta\eta\zeta\zeta} + \alpha - \alpha F^0 - \alpha\eta F^0_{\eta}\right) \\ &+ l_d \xi e^{\xi}\left(-F^0_{\tau} + F^1_{\eta\eta} + F^1_{\zeta\zeta} - (F^0_{\eta})^2 - (F^0_{\zeta})^2 + F^0_{\eta\eta\eta\eta} + F^0_{\zeta\zeta\zeta\zeta} + 2F^0_{\eta\eta\zeta\zeta}\right) \\ &+ l_D \xi e^{\xi}\left(\alpha - \alpha F^0 - \alpha\eta F^0_{\eta}\right) \\ &+ l_d \xi^2 e^{\xi}\left(-F^0_{\eta\eta\eta\eta} - F^0_{\zeta\zeta\zeta\zeta} - 2F^0_{\eta\eta\zeta\zeta} + l_d \frac{\partial^2 \theta_1}{\partial \xi^2}\right), \qquad \xi < 0 \\ \frac{\partial S_1}{\partial \xi} - \frac{\partial^2 S_1}{\partial^2 \xi^2} &= -l_d F^0_{\eta\eta\eta\eta} - l_d F^0_{\zeta\zeta\zeta\zeta} - 2F^0_{\eta\eta\zeta\zeta}, \qquad 0 < \xi < d\end{aligned}$$

$$\theta_1 = 0 \qquad S_1 = 0 \qquad R_1 = 0$$

$$\left[\frac{\partial \theta_1}{\partial \xi}\right] = -l_d \left[\frac{\partial S_1}{\partial \xi}\right] \qquad \left[\frac{\partial \theta_1}{\partial \xi}\right] = -l_e \left[\frac{\partial R_1}{\partial \xi}\right]$$

$$\left[\frac{\partial\theta_1}{\partial\xi}\right] = \frac{(l_e - l_d)(F_\eta^2 + F_\zeta^2) + 2(R_1 - S_1) - 2S_0 + 2R_0 + l_d R_1 - l_e S_1}{2(l_e - l_d)}.$$

A solution can now be constructed yielding the following:

$$\theta_1 = \begin{cases} \xi e^\xi \left(F^0_{\eta\eta\eta\eta} + F^0_{\zeta\zeta\zeta\zeta} + 2F^0_{\eta\eta\zeta\zeta} - F^0_\tau + F^1_{\eta\eta} + F^1_{\zeta\zeta} - (F^0_\eta)^2 - (F^0_\zeta)^2\right) \\ +\xi e^\xi \left(\alpha - \alpha F^0 - \alpha\eta F^0_\eta\right) - \frac{1}{2}(F^0_{\eta\eta\eta\eta} + F^0_{\zeta\zeta\zeta\zeta} + 2F^0_{\eta\eta\zeta\zeta})\xi^2 e^\xi & \xi < 0 \\ \\ 0 & 0 < \xi < d, \end{cases}$$

$$S_1 = \begin{cases} l_d e^\xi(-5F^0_{\eta\eta\eta\eta} - 5F^0_{\zeta\zeta\zeta\zeta} - 10F^0_{\eta\eta\zeta\zeta} - F^1_{\eta\eta} - F^1_{\zeta\zeta}) \\ -l_d\xi e^\xi(F^0_\tau + (F^0_\eta)^2 + (F^0_\zeta)^2 + 3F^0_{\eta\eta\zeta\zeta} + 3F^0_{\zeta\zeta\zeta\zeta} + 6F^0_{\eta\eta\zeta\zeta} - \alpha + \alpha F^0 + \alpha\eta F^0_\eta) \\ +l_d\xi^2 e^\xi \left(F^0_\tau + (F^0_\eta)^2 + (F^0_\zeta)^2 - F^1_{\eta\eta} - F^1_{\zeta\zeta} - \frac{3}{2}F^0_{\eta\eta\eta\eta} - \frac{3}{2}F^0_{\zeta\zeta\zeta\zeta} - 3F^0_{\eta\eta\zeta\zeta}\right) \\ +l_d\xi^2 e^\xi(-\alpha + \alpha F^0 + \alpha\eta F^0_\eta) \\ +l_d\xi^3 e^\xi \frac{1}{2}(F^0_{\eta\eta\eta\eta} + F^0_{\zeta\zeta\zeta\zeta} + 2F^0_{\eta\eta\zeta\zeta}) & \xi < 0 \\ \\ l_d(-5F^0_{\eta\eta\eta\eta} - 5F^0_{\zeta\zeta\zeta\zeta} - 10F^0_{\eta\eta\zeta\zeta} - F^1_{\eta\eta} - F^1_{\zeta\zeta}) \\ -l_d\xi(F^0_{\eta\eta\eta\eta} + F^0_{\zeta\zeta\zeta\zeta} + 2F^0_{\eta\eta\zeta\zeta}) & 0 < \xi < d \end{cases}$$

We can now apply the last jump condition of the order $O(\epsilon^2)$ system, and obtain the

desired evolution equation.

$$\left[\frac{\partial\theta_1}{\partial\xi}\right] = \frac{(l_e - l_d)((F_\eta^0)^2 + (F_\zeta^0)^2) + 2(R_1 - S_1) - 2S_0 + 2R_0 + l_d R_1 - l_e S_1}{2(l_e - l_d)}$$

and obtain the desired evolution equation.

$$\left(-F^0_{\eta\eta\eta\eta} - F^0_{\zeta\zeta\zeta\zeta} - 2F^0_{\eta\eta\zeta\zeta} + F^0_\tau - F^1_{\eta\eta} - F^1_{\zeta\zeta} + (F^0_\eta)^2 + (F^0_\zeta)^2 - \alpha + \alpha F^0 + \alpha\eta F^0_\eta\right)$$
$$(2l_e - 2l_d) =$$

$$(l_e - l_d)\left((F^0_\eta)^2 + (F^0_\zeta)^2\right) + 2l_E(-F^1_{\eta\eta} - F^1_{\zeta\zeta} - 5F^0_{\eta\eta\eta\eta} - 5F^0_{\zeta\zeta\zeta\zeta} - 10F^0_{\eta\eta\zeta\zeta})$$
$$-2l_d(-F^1_{\eta\eta} - F^1_{\zeta\zeta} - 5F^0_{\eta\eta\eta\eta} - 5F^0_{\zeta\zeta\zeta\zeta} - 10F^0_{\eta\eta\zeta\zeta}) - 2l_E(F^0_{\eta\eta} + F^0_{\zeta\zeta} + \alpha)$$
$$+2l_d(F^0_{\eta\eta} + F^0_{\zeta\zeta} + \alpha).$$

Finally, this can be reduced to its final form given by:

$$F^0_\tau + F^0_{\eta\eta} + F^0_{\zeta\zeta} + 4F^0_{\eta\eta\eta\eta} + 4F^0_{\zeta\zeta\zeta\zeta} + 8F^0_{\eta\eta\zeta\zeta} + \frac{1}{2}(F^0_\eta)^2 + \frac{1}{2}(F^0_\zeta)^2 \quad +$$
$$\alpha F^0 + \alpha\eta F^0_\eta \quad = \quad 0 \qquad (3.38)$$

which can be written in the more convenient form

$$F_\tau + \nabla^2 F + 4\nabla^4 F + \frac{1}{2}|\nabla F|^2 + \alpha\partial_\eta(\eta F) \quad = \quad 0. \qquad (3.39)$$

The above evolution equation is identical to that found using the single-reactant theory. Even though some portions of the flame burn rich while others burn lean, the imposed jump conditions (2.63a), (2.63b) reduce to the identical expression using the above scalings. This is a consequence of examining the weak strain rate limit for which the flame is essentially that of a planar flame in uniform flow. As a result, the flame dynamics are not modified despite the local differences in mixture composition across the front.

3.3 Trailing diffusion flame

The analysis of the previous section has demonstrated that some regions of flame can burn rich, while neighboring regions can burn lean. Since the temperature remains close to its adiabatic value behind the flame, a diffusion flame can exist along the interface where fuel and oxidant come together. For configurations where this occurs a complete description of the burned region, including the diffusion flame is needed.

We have been mostly concerned with uniformly strained flames for which the same species leaks through along the entire flame surface and thus no diffusion flame will emerge. However, we outline here the basic methodology for analyzing the burned region for future studies where diffusion flames can be expected to develop.

The governing equations are

$$\rho\frac{DT}{Dt} - \nabla^2 T = \frac{Q^2 q^2}{2(2+\phi)\epsilon^3}\rho^2 Y_E Y_D e^{\frac{E}{R\hat{T}_u}(\frac{1}{T_a}-\frac{1}{T})}, \tag{3.40}$$

$$\rho\frac{DY_D}{Dt} - \nabla^2 Y_D = \frac{-Q^2 q}{2(2+\phi)\epsilon^3}\rho^2 Y_E Y_D e^{\frac{E}{R\hat{T}_u}(\frac{1}{T_a}-\frac{1}{T})}, \tag{3.41}$$

$$\rho\frac{DY_E}{Dt} - \nabla^2 Y_E = -\nu\frac{Q^2 q}{2(2+\phi)\epsilon^3}\rho^2 Y_E Y_D e^{\frac{E}{R\hat{T}_u}(\frac{1}{T_a}-\frac{1}{T})}. \tag{3.42}$$

where we have used the expession for adiabatic flame speed found in section 2.1.3.

The procedure follows closely the Burke-Schumann analysis of a diffusion flame at the mouth of a tube in a duct, [1]. The premixed flame surface plays the role of the mouth of the tube. Fuel emerges on one side, oxidant on the other, and a diffusion flame emanates from the stoichiometric point.

Similar to the Burke-Schumann analysis, the following assumptions are made:

(a) a uniform flow is assumed.

(b) axial diffusion is negligible compared with diffusion in the transverse directions.

(c) reaction is confined to a sheet.

The present analysis differs from that in [1] in these important ways:

(i) the boundary of the burned region, i.e. the premixed flame surface, $x = f(y)$, is not planar.

(ii) the distribution of species on either side is not uniform; rather it is determined by analysis of the premixed flame.

(iii) the temperature is everywhere within $O(\epsilon)$ of its adiabatic value, and both species appear in $O(\epsilon)$ quantities.

Let x, y denote the axial and transverse coordinates respectively, so that the premixed flame surface lies at $x = f(y)$, and the burned region is given by $x > f(y)$ as in figure 3.17.

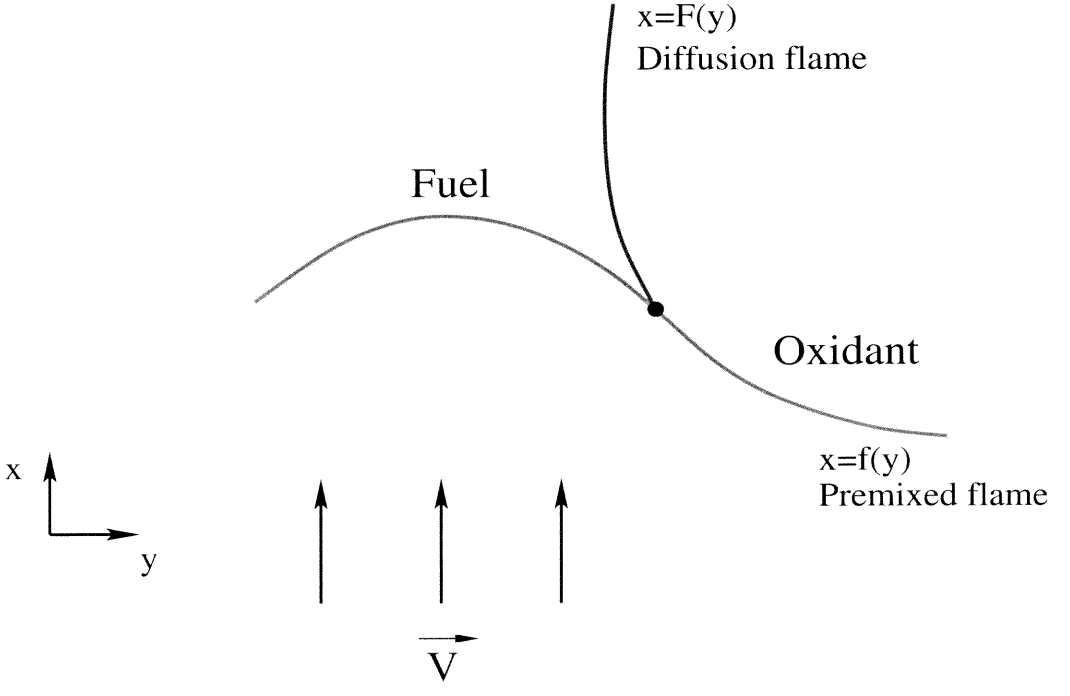

Figure 3.17: Schematic representation of the trailing of a diffusion flame

Upon expanding

$$T = T_a + \epsilon\theta \qquad Y_D = \epsilon y_D \qquad Y_E = \epsilon y_E,$$

the steady form of (3.40)-(3.42) becomes

$$\frac{\partial\theta}{\partial x} - \frac{\partial^2\theta}{\partial y^2} = \frac{q^2}{2(2+\phi_1)\epsilon^2}\, y_E\, y_D\, e^{\theta}, \tag{3.43}$$

$$\frac{\partial y_D}{\partial x} - \frac{\partial^2 y_D}{\partial y^2} = \frac{-q^2}{2(2+\phi_1)\epsilon^2}\, y_E\, y_D\, e^{\theta}, \tag{3.44}$$

$$\frac{\partial y_E}{\partial x} - \frac{\partial^2 y_E}{\partial y^2} = \frac{q^2\nu}{2(2+\phi_1)\epsilon^2}\, y_E\, y_D\, e^{\theta}. \tag{3.45}$$

The main objectives here are to determine the shape of the diffusion flame, $x = F(y)$, and to analyze the extinction behavior. Upon introducing the parameter Z given by $\omega = \frac{y_E}{\nu} - y_D$ we combine (3.44) and (3.45) to obtain

$$Z_x - Z_{zz} = 0 \tag{3.46}$$

This is to be solved subject to the appropriate boundary conditions at the premixed surface. At the diffusion flame surface, both y_E and y_D vanish and so the flame shape is obtained by simply setting $Z = 0$.

To analyse the extinction characteristics of the diffusion flame, local analysis of the reaction zone is needed. The results will depend, through matching, on the manner in which the species leak through the premixed flame for a given configuration.

The analysis follows closely that of Liñán [19]. By introducing a stretched variable in the vicinity of the diffusion flame, the resulting reaction-diffusion equaitons can be integrated resulting in explicit criteria for extinction. Again, the results are obtained by matching to the temperature and species profiles in the outer region on

either side of the diffusion flame, which in turn are determined by conditions at the premixed front.

CHAPTER 4

CONCLUSIONS AND SUGGESTIONS FOR FUTURE RESEARCH

In this work, we have derived a new theory of premixed flames in near-stoichiometric mixtures. The new model is a diffusional thermal model obtained in a rational way from the original system of equations given by the transport of heat and species equations, as well as the hydrodynamic equations from fluid dynamics. The method of large activation asymptotics was used, and the weak thermal expansion limit was considered to obtain a new system, given by (2.57)-(2.64). This model is decoupled from the equations of hydrodynamics and it is valid over a range of mixture strength. Once derived, the model was used to study the behavior of planar flames in strained flows.

The major differences between our model and the single reactant theory are: (a) there are now two Lewis numbers that can significantly change the dynamics of our problem, provided the two species diffuse at unequal rates, (b) a new parameter is of great importance, the equivalence ratio (Φ), which affects fundamental properties of the flame, such as instabilities and extinction phenomena, (c) the locally deficient component is not necessarily consumed behind the flame, but rather it is possible for the initially excess species to be locally deficient and hence, consumed by the reaction, and (d) as a result of this possibility there are now two jump conditions for the temperature gradient.

For off-stoichiometric mixtures, our system reduces to the single reactant theory, showing that our model describes the flame behavior in conditions far removed from stoichiometry as well. When conditions are closer to stoichiometry, we can capture new dynamics as the flame response depends in a non-trivial way on which of the two species is consumed.

To illustrate this phenomena we investigated the extinction of strained flames, and in particular a stretched flame in stagnation point flow. We were able to construct complete steady solutions that describe the flame response and depend on the values of equivalence ratio, Lewis numbers, and strain rate. Results show that the flame position can decrease monotonically with strain rate suggesting that the flame can be pushed all the way to the wall, or the response is double-valued suggesting extinction at a finite distance from the wall. For off-stoichiometric mixtures we recover Buckmaster's results from single reactant theory, valid for very lean or very rich conditions. Also, for weakly-strained flames, we showed that the structure is essentially that of a planar flame in a uniform flow field.

For near-stoichiometric strained flames, many of the conclusions of the single-reactant theory are modified as a result of the differing diffusivities of the two species. In particular, we showed for certain specific parameter values at which the single reactant theory predicts a double-valued flame response, our theory predicts a monotonic response and no extinction point when conditions are closer to stoichiometry. The standoff distance at extinction has been calculated as a function of equivalence ratio, and results are consistent with the experimental measurements of Yamaoka and Tsuji, [17].

The model derived here paves the way for a number of future studies on flame dynamics. Thus far, only perturbed planar flames and planar flames in uniformly strained flames have been analyzed using this model. It is be of interest to study curved flames as well as strained flames that are not uniformly stretched. Of particular interest is to determine if and how flame dynamics differ along portions of the front that burn rich as opposed to to those that burn lean.

Also, it would be of interest to analyze in detail the structure of the trailing diffusion flame under conditions where concentration gradients exist along the premixed flame surface. These structures are reminiscent of triple flames which are

thought to be the mechanism by which quenched regions of turbulent diffusion flames are re-ignited. The precise conditions under which these structures develop is not yet fully understood.

Finally, it would be of interest to carry out a full numerical treatment of the systems considered here to validate our conclusions. This would permit a more realistic description of chemistry and the flow field.

BIBLIOGRAPHY

[1] F. A. Williams, *Combustion Theory.* Benjamin Cummings. Menlo Park, California, 2nd ed., 1985.

[2] A. R. Burgess and L. J. Molero, "Nitrogenous emissions:the role of sulphur and equivalence ratio," *American Japanese Flame Research Committees International Symposium*, 1998.

[3] L. D. Landau, "On the theory of slow combustion," *Acta Physicochimica URSS*, vol. 19, 1944.

[4] G. Darrieus, "Propagation d'un front de flamme de deflagration par developpement spontane de la turbulence. presented at the int. congr. appl. mech., 6th, paris, 1946," 1938.

[5] P. Clavin and F. A. Williams, "Effects of molecular diffusion and of thermal expansion on the structure and dynamics of premixed flames in turbulent flows of large scales and low intensity," *Journal of Fluid Mechanics*, vol. 116, 1982.

[6] M. Matalon and B. J. Matkowsky, "Flames as gasdynamic discontinuities," *Journal of Fluid Mechanics*, vol. 124, pp. 239–259, 1982.

[7] B. J. Matkowsky and G. I. Sivashinsky, "An asymptotic derivation of two models in flame theory associated with the constant density approximation," *SIAM Journal of Applied Mathematics*, vol. 37, p. 686, 1979.

[8] G. I. Sivashinsky, "On a distorted flame front as a hydrodynamic discontinuity," *Acta Astronautica*, vol. 3, 1976.

[9] A. K. Sen and G. S. S. Ludford, "The near-stoichiometric behavior of combustible mixtures, part I: Diffusion of the reactants," *Combustion Science and Technology*, vol. 21, p. 15, 1979.

[10] T. Mitani, "Propagation velocities of two-reactant flames," *Combustion Science and Technology*, vol. 21, p. 175, 1980.

[11] G. Joulin and T. Mitani, "Linear stability analysis of two-reactant flames," *Combustion and Flame*, vol. 40, p. 235, 1981.

[12] G. I. Sivashinsky, "On flame propagation under conditions of stoichiometry," *SIAM Journal of Applied Mathematics*, vol. 39, p. 67, 1980.

[13] T. L. Jackson, "Effect of thermal expansion on the stability of two-reactant flames," *Combustion Science and Technology*, vol. 53, p. 51, 1987.

[14] C. Cui, M. Matalon, and J. K. Bechtold, "Hydrodynamic theory of near-stoichiometric premixed flames," *Submitted to the Journal of Fluid Mechanics*, 2001.

[15] J. K. Bechtold and M. Matalon, "Effects of stoichiometry on stretched premixed flames," *Combustion and Flames*, vol. 119, pp. 217–232, 1999.

[16] J. D. Buckmaster, "The quenching of a deflagration wave held in front of a bluff body," *17th International Symposium on Combustion*, 1979.

[17] I. Yamaoka and H. Tsuji, "An anomalous behavior of methane-air and methane-hydrogen-air flames diluted with nitrogen in a stagnation flow," *Twenty-Fourth Symposium (International) on Combustion/The Combustion Institute*, pp. 145–152, 1992.

[18] G. I. Sivashinsky, C. K. Law, and G. Joulin, "On stability of premixed flames in stagnation-point flow," *Combustion Science and Technology*, vol. 28, pp. 115–159, 1982.

[19] A. Liñán, "The asymptotic structure of counterflow diffusion flames for large activation energies," *Acta Astronautica*, vol. 1, 1974.